WP 1 Report: Catalysts Preparation

Table of Contents

1.1 Introduction 2
1.2 General information 5
1.3 Necessary Administrative and Technical Preparation 8
1.3.1 Administrative Preparation 9
1.3.2 Laboratory Safety and Environmental Preparation 10
1.3.3 Preparation of Chemicals and Electrolytes 12
1.3.4 Preparation of Experimental Equipment 13
1.3.5 Preparation of Electrode Substrates 13
1.3.6 Development of Experimental Protocols 14
1.3.7 Computational Infrastructure 15
1.3.8 Summary 15
1.4 Electrodeposition of Ni from DES-Based Electrolytes 16
1.4.1 Introduction 16
1.4.2 Preparation of the Ethaline-Based Electrolyte 18
1.4.3 Electrochemical Cell and Experimental Setup 19
1.4.4 Optimization of Electrodeposition Parameters 21
1.4.5 Influence of Temperature and Current Density 25
1.4.6 Current Efficiency of Ni Electrodeposition 28
1.4.7 Deposition Rate 30
1.4.8 Selection of Optimal Conditions for Subsequent Ni/MoS_2 Composite Electrodeposition 33
1.4.9 Summary 37
1.5 Electrodeposition of Ni/MoS_2 composite coatings for catalytic HER 38
1.5.1 Preparation of a colloidal Ethaline-based electrolyte for the electrodeposition of MoS_2-containing Ni composites 38
1.5.1.1 Synthesis of MoS_2 in Ethaline-based electrolytes 39

1.5.1.2 Synthesis, isolation, and re-dispersion of MoS_2 nanoparticles in Ethaline-based electrolyte for Ni/MoS_2 composite electrodeposition 41
1.5.1.3 Preparation of Ni–MoS_2 containing electrolyte using commercial MoS_2 powder 43
1.5.1.4 Comparison of commercial and synthesized MoS_2 powders 45
1.5.2 Electrodeposition conditions for obtaining Ni/MoS_2 composite coatings from the Ethaline-based electrolyte: influence of different factors.....49
1.6 Thermal engineering of MoFeNiP carbon electrocatalysts for efficient hydrogen evolution in acidic and alkaline media 51
1.7 Preparation of catalytically active Ni foams by the replication method.....53
1.8 Valorization of PUR foams into an efficient HER catalyst by electroless deposition and electrodeposition of Ni 57
1.9 Electrodeposition and process optimization of Ni/M-Xene composite catalytic coatings 62
1.10 Synthesis of $Ni_{1-x}Co_xS$ Electrocatalysts and Electrode Fabrication 69

1.1 Introduction

The transition towards a carbon-neutral economy requires the development of sustainable technologies for clean energy conversion and storage. Among the numerous renewable energy carriers currently under investigation, hydrogen has emerged as one of the most promising alternatives to fossil fuels due to its high gravimetric energy density, zero carbon emissions during utilization, and compatibility with existing and future energy infrastructures. In particular, hydrogen produced by water electrolysis powered by renewable electricity ("green hydrogen") is considered a cornerstone technology for achieving the climate neutrality targets established by the European Green Deal and the European Hydrogen Strategy.

Despite remarkable advances in electrolyser technology, the widespread implementation of water electrolysis remains limited by the relatively high capital

and operational costs associated with electrocatalysts. Commercial alkaline electrolyzers still rely on noble-metal-based catalysts or expensive manufacturing routes, which significantly increase the overall cost of hydrogen production. Consequently, the development of highly active, stable, earth-abundant, and economically viable electrocatalysts for the hydrogen evolution reaction (HER) has become one of the major scientific and technological priorities in modern electrochemistry and materials science.

Among transition-metal-based catalysts, nickel-based materials have attracted considerable attention owing to their excellent corrosion resistance in alkaline media, relatively low cost, and favorable catalytic activity. Nevertheless, pure nickel still exhibits higher HER overpotentials than noble metals, motivating extensive research into alloying strategies, heterostructure engineering, composite electrodeposition, and nanostructuring approaches capable of increasing the density of catalytically active sites while improving charge transfer and long-term stability.

Recent developments have demonstrated that combining nickel with molybdenum-containing compounds, particularly transition metal dichalcogenides such as molybdenum disulfide (MoS_2), offers significant opportunities for enhancing catalytic activity. MoS_2 possesses abundant edge-active sites for hydrogen adsorption, whereas nickel provides excellent electrical conductivity and mechanical stability. The formation of Ni/MoS_2 composite catalysts therefore represents a promising strategy for achieving synergistic catalytic effects that outperform the individual components. Furthermore, introducing three-dimensional porous substrates, including nickel foams and carbon-based foams, substantially increases the electrochemically active surface area, facilitates gas evolution, improves electrolyte transport, and enhances catalyst durability.

A key innovation of the DEMADES project lies in the application of deep eutectic solvents (DESs) as environmentally benign electrolytes and reaction media

for catalyst synthesis. DESs possess several advantages over conventional aqueous electrolytes, including a wide electrochemical stability window, negligible vapor pressure, high ionic conductivity, excellent solvating ability for metal salts, and intrinsic compatibility with Green Chemistry principles. Their unique physicochemical properties suppress parasitic hydrogen evolution during electrodeposition, enabling improved control over coating composition, morphology, crystallinity, and nanostructure formation. In addition, the higher viscosity of DESs contributes to improved stability of particle suspensions, making these media particularly attractive for composite electrodeposition involving nanosized catalytic particles.

The first work package (WP1) of the DEMADES project is therefore dedicated to the preparation and optimization of advanced HER electrocatalysts using environmentally friendly synthesis methodologies based primarily on DES-containing systems. The work package combines electrochemical deposition, electroless deposition, chemical synthesis of nanomaterials, foam replication technologies, and computational materials screening to establish efficient preparation routes for next-generation hydrogen evolution catalysts.

WP1 encompasses several complementary research activities. Initially, optimized DES electrolytes are prepared together with the necessary laboratory infrastructure and safety procedures. Nickel electrodeposition from various DES formulations is subsequently investigated as a model system for understanding metal nucleation and growth under non-aqueous conditions. Parallel efforts focus on the synthesis of catalytically active MoS_2 nanoparticles with controlled morphology, phase composition, and defect density. These nanoparticles are subsequently incorporated into nickel matrices through composite electrodeposition to produce Ni/MoS_2 coatings with enhanced HER performance.

To further increase catalyst surface area and mass transport characteristics, three-dimensional nickel foams are fabricated using sacrificial polymer templates through replication methods. In parallel, commercially available polyurethane foams are transformed into electrically conductive metallic scaffolds via sequential electroless and electrochemical nickel deposition. Finally, artificial intelligence (AI) and machine learning (ML) methodologies are employed to accelerate catalyst discovery by computationally screening different classes of molybdenum-based compounds, including MoS_2, $MoSe_2$, MoP, Mo_2N, Mo_2C, and MoB, while evaluating the influence of defect engineering, heterointerface formation, and dopant incorporation on catalytic performance.

Collectively, the activities performed within WP1 establish the scientific and technological foundation for the subsequent work packages devoted to catalyst characterization, electrochemical evaluation, mechanistic investigations, and optimization. The generated knowledge contributes directly to the development of sustainable catalyst preparation strategies that combine high catalytic efficiency with environmentally responsible manufacturing processes, thereby supporting the broader objectives of decarbonization and green hydrogen production.

1.2 General information

Work Package 1 (WP1), entitled "Catalysts Preparation", constitutes the initial experimental phase of the DEMADES project and focuses on the synthesis, optimization, and preliminary evaluation of advanced electrocatalytic materials for the hydrogen evolution reaction in alkaline media. The primary objective of WP1 is to establish reliable, reproducible, and environmentally sustainable preparation protocols for a wide range of nickel-based catalysts fabricated using deep eutectic solvents and complementary green synthesis techniques.

The preparation strategy adopted within WP1 combines several state-of-the-art approaches in materials science, electrochemistry, nanotechnology, and computational materials engineering. These approaches include electrochemical deposition, electroless deposition, nanoparticle synthesis, three-dimensional foam fabrication, and artificial intelligence-assisted catalyst design. The integration of these methodologies enables systematic investigation of the relationships between synthesis conditions, catalyst composition, nanostructure, morphology, and electrocatalytic performance.

The catalyst preparation activities are based on several fundamental design principles:

- utilization of environmentally friendly deep eutectic solvents as alternatives to conventional aqueous electrolytes;
- development of nanostructured nickel-based catalytic coatings with enhanced active surface area;
- incorporation of catalytically active molybdenum compounds into metallic matrices;
- fabrication of three-dimensional porous catalyst architectures;
- minimization of noble metal utilization through rational catalyst design;
- implementation of computational screening tools to accelerate materials discovery.

The research performed within WP1 addresses several classes of catalytic materials, including pure nickel coatings, Ni/MoS_2 composite coatings, metallic foams, foam-supported catalysts, and transition-metal compounds identified through AI-assisted screening. The investigated catalyst systems are specifically selected based on their reported activity toward alkaline hydrogen evolution, long-term electrochemical stability, abundance of constituent elements, and compatibility with scalable manufacturing technologies.

Deep eutectic solvents represent the principal synthesis medium throughout the work package. DESs based on choline chloride combined with hydrogen bond donors such as ethylene glycol, urea, glycerol, or related compounds offer numerous advantages compared to conventional aqueous electrolytes. These include:

- ✓ extended electrochemical stability windows;
- ✓ suppression of parasitic hydrogen evolution during electrodeposition;
- ✓ improved control of nucleation and crystal growth;
- ✓ enhanced suspension stability for nanoparticle codeposition;
- ✓ lower environmental impact;
- ✓ biodegradability;
- ✓ simplified waste management;
- ✓ compatibility with Green Chemistry principles.

The preparation methodologies implemented during WP1 include both bottom-up and top-down fabrication strategies. Electrochemical deposition enables precise control of coating thickness, composition, grain size, and microstructure by adjusting deposition potential, current density, electrolyte composition, temperature, and deposition time. Electroless deposition provides uniform metallization of electrically non-conductive porous substrates, particularly polyurethane foams used as sacrificial templates or catalyst supports. Chemical synthesis routes are employed for preparing nanoscale MoS_2 with controlled crystal structure and morphology suitable for composite electrodeposition.

A significant component of WP1 is devoted to the fabrication of three-dimensional catalyst architectures. Porous nickel foams produced by replication methods exhibit exceptionally high specific surface areas, interconnected pore networks, and excellent mechanical stability, all of which contribute to improved gas evolution kinetics and enhanced catalyst utilization during HER. Similarly, metallized polyurethane foams provide lightweight conductive scaffolds suitable for

the deposition of catalytically active layers while maintaining highly accessible porous structures.

In addition to experimental synthesis, WP1 incorporates modern computational approaches for catalyst design. Artificial intelligence and machine learning techniques are employed to analyze large datasets of experimental and theoretical catalytic descriptors, enabling rapid identification of promising molybdenum-based compounds and optimization strategies. Particular attention is devoted to understanding the influence of crystal defects, heterostructure interfaces, elemental doping, and electronic structure modifications on HER activity.

The activities carried out during WP1 generate a comprehensive library of catalyst materials with systematically varied compositions, morphologies, and nanostructures. These materials constitute the basis for subsequent structural characterization, electrochemical testing, durability evaluation, mechanistic investigations, and optimization performed in later work packages.

Overall, WP1 establishes the technological platform for sustainable catalyst fabrication within the DEMADES project by integrating green chemistry principles, advanced electrochemical synthesis, nanomaterials engineering, porous material fabrication, and data-driven materials discovery. The knowledge generated during this work package provides the necessary scientific foundation for developing efficient, durable, and economically viable HER electrocatalysts capable of supporting large-scale green hydrogen production.

1.3 Necessary Administrative and Technical Preparation

Successful implementation of the catalyst synthesis activities described in Work Package 1 required comprehensive administrative, organizational, and technical preparation before commencing experimental work. Since the work package combines electrochemical synthesis, chemical synthesis of nanomaterials,

electroless deposition, foam replication technologies, and artificial intelligence (AI)-assisted materials design, careful planning was essential to ensure reproducibility, safety, regulatory compliance, and efficient utilization of research infrastructure. The preparatory activities established the experimental framework for all subsequent investigations and ensured that laboratory work could be conducted in accordance with internationally accepted standards of scientific research.

1.3.1 Administrative Preparation

The administrative preparation focused on establishing the organizational structure necessary for efficient implementation of WP1 and coordination among project partners. At the beginning of the reporting period, responsibilities of individual research groups and researchers were defined according to their expertise in electrochemistry, materials science, surface engineering, nanotechnology, computational modelling, and advanced characterization methods. The work package objectives, milestones, expected deliverables, and reporting procedures were reviewed and harmonized with the overall project management plan to ensure consistency with the DEMADES project objectives.

Regular communication channels between the participating institutions were established through scheduled online meetings, technical consultations, and internal workshops. These meetings facilitated the exchange of scientific knowledge, discussion of experimental procedures, monitoring of project progress, and coordination of shared research activities. Standard procedures for documentation of experimental data, preparation of laboratory reports, storage of electronic files, and version control of research documents were also implemented to ensure traceability and reproducibility of all experimental work.

A comprehensive research data management strategy was adopted in accordance with FAIR (Findable, Accessible, Interoperable, and Reusable) data principles.

Experimental data generated throughout WP1 are systematically archived using standardized formats, accompanied by detailed metadata describing synthesis conditions, experimental parameters, analytical methods, and sample identification. Secure institutional servers and cloud-based storage systems are utilized for data backup, while access rights are managed according to project responsibilities and intellectual property requirements.

Ethical considerations and intellectual property management procedures were also established before initiating laboratory activities. Confidential information concerning novel catalyst compositions, synthesis procedures, and potentially patentable technologies is managed according to institutional regulations and collaboration agreements between project partners. At the same time, scientific transparency is maintained through detailed documentation of experimental procedures and planned dissemination of non-confidential research outcomes in accordance with Open Science principles.

Administrative preparation also included procurement planning and inventory management for chemicals, consumables, laboratory equipment, and safety supplies. Supplier qualification, ordering schedules, storage conditions, and quality verification procedures were organized to minimize delays in experimental work and ensure uninterrupted availability of required materials.

1.3.2 Laboratory Safety and Environmental Preparation

Considering the extensive use of chemical reagents, electrochemical equipment, elevated temperatures, and nanomaterials, significant attention was devoted to laboratory safety before experimental activities were initiated.

Comprehensive risk assessments were prepared for all planned experimental procedures, including:

- preparation of deep eutectic solvents;

- electrochemical deposition processes;
- synthesis of MoS_2 nanoparticles;
- electroless deposition;
- preparation of metallic foams;
- handling of nanomaterials;
- alkaline electrochemical testing.

Laboratory personnel and involved researchers received training in chemical safety, handling of corrosive chemicals, waste management, operation of electrochemical instrumentation, and emergency response procedures. Particular attention was devoted to handling concentrated alkaline electrolytes, transition-metal salts, sulfur-containing compounds, reducing agents, and nanoparticles.

Although deep eutectic solvents are considerably safer than many conventional organic solvents, their preparation and handling were performed under controlled laboratory conditions. Material Safety Data Sheets (MSDS) for all chemicals were collected and made readily accessible to all project participants. Appropriate personal protective equipment (PPE), including laboratory coats, protective gloves, safety glasses, and face shields where necessary, was mandatory throughout all experimental procedures.

Environmental sustainability formed an integral part of the laboratory preparation. The selection of DES-based electrolytes reflects the project's commitment to Green Chemistry by minimizing the use of volatile organic solvents and hazardous chemicals. Procedures for waste segregation, collection, neutralization, recycling, and disposal were established according to institutional environmental regulations and national legislation.

1.3.3 Preparation of Chemicals and Electrolytes

An essential part of the technical preparation involved procurement and verification of high-purity chemicals required for catalyst synthesis.

Analytical-grade reagents were obtained from certified suppliers, including:

- choline chloride;
- ethylene glycol;
- urea;
- glycerol;
- nickel salts;
- molybdenum precursors;
- sulfur-containing reagents;
- reducing agents;
- supporting electrolytes;
- alkaline solutions for electrochemical testing.

Each chemical batch was inspected upon delivery, and storage conditions were established according to manufacturer recommendations regarding temperature, humidity, and light exposure.

Preparation protocols for deep eutectic solvents were optimized before commencing electrodeposition experiments. Particular attention was devoted to controlling the molar ratio of hydrogen bond donors and acceptors, preparation temperature, mixing conditions, moisture content, viscosity, and storage stability. Standardized procedures were developed to ensure excellent reproducibility between individual electrolyte batches.

Model aqueous electrolytes required for catalyst evaluation, including potassium hydroxide solutions for HER measurements, were also prepared using high-purity deionized water with resistivity exceeding 18 MΩ·cm to minimize contamination.

1.3.4 Preparation of Experimental Equipment

Reliable catalyst synthesis requires properly calibrated and maintained instrumentation. Therefore, all experimental equipment intended for WP1 activities underwent inspection, servicing, and calibration before beginning experimental work.

Electrochemical workstations, including potentiostats and galvanostats, were purchased and tested using standard electrochemical systems to verify current accuracy, potential control, impedance response, and data acquisition performance. Electrode holders, electrochemical cells, thermostatic baths, magnetic stirrers, and temperature controllers were inspected to ensure stable operating conditions during long-term deposition experiments.

Auxiliary laboratory equipment including analytical balances, pH meters, conductivity meters, ultrasonic baths, drying ovens, vacuum systems, furnaces, and mechanical polishing equipment were calibrated according to institutional quality assurance procedures.

For nanoparticle synthesis and foam preparation, additional laboratory equipment including glass reactors, reflux systems, filtration units, vacuum drying systems, and ultrasonic dispersers were prepared and tested before experimental implementation.

1.3.5 Preparation of Electrode Substrates

Since substrate quality significantly influences coating adhesion, nucleation behavior, and catalytic performance, standardized substrate preparation protocols were developed before initiating electrodeposition experiments.

Nickel substrates, metallic foams, polyurethane foams, and other conductive materials were subjected to systematic surface preparation consisting of:

- mechanical polishing where applicable;
- ultrasonic degreasing;

- alkaline cleaning;
- acid activation;
- rinsing with ultrapure water;
- drying under controlled conditions.

Special attention was devoted to the preparation of nickel foams because their three-dimensional porous architecture requires complete removal of contaminants while preserving structural integrity. Surface activation procedures were optimized to maximize coating adhesion and ensure homogeneous catalyst deposition throughout the foam volume.

Commercial polyurethane foams intended for metallization were cleaned, cut into standardized dimensions, and characterized before electroless nickel deposition. The pore size distribution, density, and mechanical properties of the polymer templates were evaluated to ensure reproducible fabrication of porous metallic structures.

1.3.6 Development of Experimental Protocols

Before experimental synthesis, detailed standard operating procedures (SOPs) were prepared for all laboratory processes included within WP1. These protocols define every experimental step, including reagent preparation, electrolyte composition, deposition parameters, cleaning procedures, sampling intervals, post-treatment methods, and characterization requirements.

Specific protocols were developed for:

- preparation of deep eutectic solvents;
- electrochemical deposition of nickel;
- synthesis of MoS_2 nanoparticles;
- composite electrodeposition of Ni/MoS_2 coatings;
- electroless nickel deposition;

- preparation of nickel foams by replication;
- metallization of polyurethane foams;
- electrochemical HER testing;
- sample storage and labeling.

The use of standardized experimental procedures minimizes operator-dependent variability and significantly improves reproducibility between independent experiments and collaborating laboratories.

1.3.7 Computational Infrastructure

In parallel with laboratory preparation, computational resources required for artificial intelligence and machine learning studies were established. Dedicated workstations equipped with scientific computing software, materials databases, and machine learning libraries were configured for catalyst screening and data analysis.

Data processing environments were prepared using programming languages such as Python together with scientific libraries for numerical analysis, visualization, and machine learning. Materials databases containing crystallographic information, electronic structure descriptors, catalytic performance data, and published HER datasets were collected to support computational investigations of molybdenum-based catalysts.

1.3.8 Summary

The administrative and technical preparation completed prior to experimental work established a robust foundation for the successful implementation of Work Package 1. Comprehensive planning of laboratory infrastructure, safety procedures, chemical procurement, equipment calibration, substrate preparation, standardized operating protocols, data management, and computational resources ensures that all catalyst synthesis activities are performed under controlled, reproducible, and environmentally responsible conditions. These preparatory activities significantly

reduce experimental uncertainty, improve research efficiency, and facilitate the production of reliable scientific results that will support the subsequent development and evaluation of advanced electrocatalysts for sustainable hydrogen evolution.

1.4 Electrodeposition of Ni from DES-Based Electrolytes

1.4.1 Introduction

Nickel is one of the most extensively investigated transition metals for the HER in alkaline electrolytes owing to its relatively low cost, high electrical conductivity, excellent corrosion resistance, and satisfactory catalytic activity. Although platinum remains the benchmark catalyst for hydrogen production, its scarcity and high price severely limit its large-scale application in industrial alkaline water electrolysis. Consequently, considerable research efforts have focused on developing nickel-based electrocatalysts capable of approaching the catalytic performance of noble metals while maintaining low production costs and high long-term stability.

Electrodeposition represents one of the most attractive techniques for manufacturing nickel electrocatalysts because it enables precise control over coating thickness, composition, crystallographic orientation, surface roughness, and nanostructure through simple adjustment of electrochemical parameters. Compared with vacuum deposition techniques, electrochemical synthesis is inexpensive, scalable, energy-efficient, and readily applicable to substrates of complex geometry, including porous metallic foams and three-dimensional architectures. These advantages have established electrodeposition as one of the principal fabrication routes for modern electrocatalysts intended for alkaline water electrolysis.

Traditionally, nickel electrodeposition has been performed using aqueous electrolytes, particularly Watts-type baths containing nickel sulfate, nickel chloride, and boric acid. Although these electrolytes have been widely employed in industrial electroplating for decades, their application in catalyst preparation suffers from

several important limitations. During deposition at sufficiently negative potentials, hydrogen evolution competes with nickel reduction, resulting in decreased current efficiency, increased internal stresses, formation of pores and cracks, deterioration of coating adhesion, and limited control over crystal growth. Furthermore, aqueous electrolytes restrict the electrochemical window available for deposition and often require additives that may pose environmental or health concerns.

Deep eutectic solvents (DESs) have recently emerged as a promising alternative to conventional aqueous electrolytes for electrodeposition of metals and alloys. DESs are formed by mixing a hydrogen bond acceptor and hydrogen bond donor in appropriate molar ratios, producing liquids with melting temperatures significantly lower than those of their individual components. These liquids combine many advantages desirable for electrochemical synthesis, including negligible vapor pressure, excellent chemical stability, high ionic conductivity, wide electrochemical windows, relatively low toxicity, and straightforward preparation from inexpensive and biodegradable components.

Among numerous DES formulations, Ethaline, consisting of choline chloride and ethylene glycol in a 1:2 molar ratio, has attracted considerable attention for electrodeposition applications. The solvent possesses moderate viscosity, high metal salt solubility, good electrochemical stability, and relatively fast ionic transport compared with other DES systems. Most importantly, hydrogen evolution is considerably suppressed compared with aqueous electrolytes, allowing nickel deposition to proceed under conditions that would otherwise be dominated by parasitic gas evolution.

The reduced competition between nickel reduction and hydrogen evolution significantly improves the utilization of electrical energy for metal deposition while simultaneously providing greater flexibility in tailoring coating properties through optimization of current density, temperature, electrolyte composition, and deposition

time. Moreover, the relatively high viscosity of Ethaline contributes to excellent suspension stability, making it particularly attractive for the subsequent electrodeposition of composite coatings containing dispersed catalytic nanoparticles.

Within the DEMADES project, optimization of nickel electrodeposition from Ethaline-based electrolytes represents the fundamental step toward the development of advanced HER electrocatalysts. The resulting nickel coatings serve not only as individual catalytic materials but also as matrix materials for the incorporation of catalytically active MoS_2 nanoparticles and others described in the following section. Consequently, establishing robust electrodeposition protocols with high current efficiency, reproducible deposition rates, and excellent coating quality was considered one of the primary objectives of WP 1.

1.4.2 Preparation of the Ethaline-Based Electrolyte

The electrolyte employed for nickel electrodeposition was based on the deep eutectic solvent Ethaline, prepared by mixing choline chloride (ChCl) and ethylene glycol (EG) in a molar ratio of 1:2. The mixture was heated under continuous magnetic stirring until a homogeneous transparent liquid was obtained. Preparation was carried out at an elevated temperature (60-70 ^{o}C) to facilitate hydrogen bond formation and reduce the viscosity of the resulting solvent. Care was taken to avoid moisture contamination during preparation because excessive water uptake may alter the physicochemical properties of the electrolyte, including viscosity, conductivity, and electrochemical stability.

Following preparation of the DES, nickel chloride hexahydrate ($NiCl_2 \cdot 6H_2O$) was dissolved to provide nickel ions for electrodeposition. Boric acid was subsequently introduced into the electrolyte as a buffering additive to stabilize the local chemical environment during deposition. Finally, 30 wt.% of deionized water

was added to reduce the viscosity of the electrolyte and enhance ionic conductivity without significantly compromising the beneficial characteristics of the deep eutectic solvent.

The final electrolyte composition is summarized in Table 1.

Table 1. Composition of the Ethaline-based electrolyte used for nickel electrodeposition.

Component	Concentration
$NiCl_2 \cdot 6H_2O$	1.0 M
Boric acid	0.13 M
Additional water	30 wt.%
Ethaline (ChCl:EG = 1:2)	Balance

The selected electrolyte composition represents a compromise between several competing factors. A sufficiently high nickel-ion concentration is required to sustain stable metal deposition throughout the experiment, whereas excessive concentrations may increase solution viscosity and promote concentration polarization. The addition of water substantially lowers viscosity and improves mass transport, while preserving the wide electrochemical window characteristic of DESs. This formulation therefore provides stable deposition conditions suitable for both pure nickel electrodeposition and subsequent preparation of composite coatings containing suspended MoS_2 nanoparticles.

1.4.3 Electrochemical Cell and Experimental Setup

Nickel electrodeposition experiments were performed in a thermostatically controlled three-electrode electrochemical cell specifically designed for studies with DESs (Fig. 1). Temperature control was achieved using a double-walled glass

reactor connected to a circulating thermostatic bath, allowing accurate regulation of electrolyte temperature throughout the deposition process.

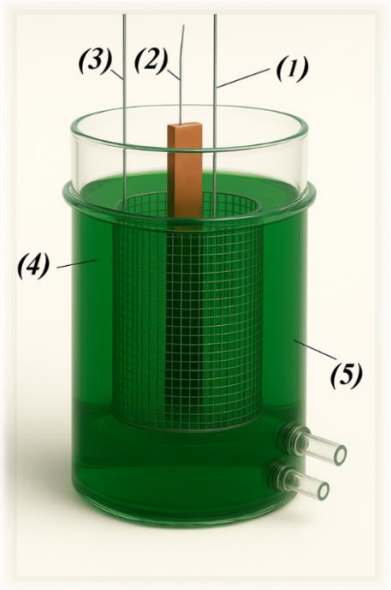


Figure 1. Schematic illustration of the thermostatically controlled three-electrode electrochemical cell used for nickel electrodeposition from the Ethaline-based deep eutectic solvent electrolyte. (1) Ag wire pseudo-reference electrode; (2) Cu working electrode (substrate for Ni deposition); (3) Ni mesh counter electrode (anode); (4) Ethaline-based nickel electrolyte; (5) double-walled jacketed glass cell connected to an external circulating thermostat for temperature control.

Copper plates with an exposed geometric surface area of 4 cm^2 served as working electrodes. Before deposition, the substrates were mechanically polished, chemically cleaned, rinsed with deionized water, degreased in ethanol, and dried under ambient laboratory conditions to ensure reproducible nucleation of nickel and adequate coating adhesion.

A nickel mesh was employed as the counter electrode. The use of a nickel anode minimizes contamination of the electrolyte by foreign metal ions while maintaining a stable concentration of nickel species during prolonged deposition experiments. Potentials were measured against a silver-wire pseudo-reference electrode immersed

directly in the Ethaline electrolyte. Since all experiments were conducted under identical electrolyte composition and temperature conditions, the pseudo-reference provided highly reproducible potential measurements suitable for comparative analysis of deposition parameters.

Galvanostatic electrodeposition was selected as the principal deposition mode because it enables precise control of metal deposition rate and facilitates systematic evaluation of current density effects on coating formation. All electrochemical experiments were performed using computer-controlled potentiostat/galvanostat instrumentation capable of continuous acquisition of current, potential, and deposition time throughout the experiments.

1.4.4 Optimization of Electrodeposition Parameters

The electrochemical synthesis of nickel coatings from DES requires careful optimization of the deposition conditions in order to achieve reproducible catalyst preparation with high deposition efficiency and suitable growth kinetics. In contrast to conventional aqueous electrolytes, where hydrogen evolution frequently limits the accessible deposition window, DES-based electrolytes provide considerably greater flexibility in controlling electrochemical reduction processes. Nevertheless, deposition parameters must be selected carefully because electrolyte viscosity, ionic mobility, mass transport, and nucleation kinetics are all strongly influenced by both temperature and applied current density.

The objective of the optimization study was therefore to identify deposition conditions that provide stable nickel electrodeposition while maintaining high current efficiency, acceptable deposition rates, and reproducible electrochemical behaviour. Since the nickel coatings prepared in this stage were intended to serve as model catalysts and as substrates for subsequent Ni/MoS_2 composite

electrodeposition, optimization was focused primarily on the electrochemical process itself rather than on detailed structural characterization.

A systematic experimental matrix was designed in which current density and electrolyte temperature were varied while maintaining all remaining deposition parameters constant. Galvanostatic electrodeposition was selected because constant-current operation enables direct investigation of the influence of current density on deposition kinetics and facilitates comparison between different experimental conditions. The deposition time was fixed at 20 minutes for all experiments, allowing direct comparison of deposition rates and current efficiencies while minimizing the influence of coating thickness on process evaluation.

The investigated experimental conditions are summarized in Table 2. Current densities ranging from 2 to 50 mA cm^{-2} were initially examined at 40 °C to determine the practical deposition window. Subsequently, a narrower range of 5–20 mA cm^{-2} was investigated at temperatures of 30, 40, 50, and 60 °C to evaluate the combined influence of thermal activation and electrochemical driving force on Ni deposition. This approach enabled identification of the most suitable operating conditions while avoiding unnecessary experiments under clearly unsuitable deposition regimes.

Table 2. Experimental conditions used for nickel electrodeposition from the Ethaline-based electrolyte.

Sample	**Current density, *i* (mA cm^{-2})**	**Temperature, *t* (°C)**	**Deposition time, *τ* (min)**
1	2	40	20
2	5	40	20
3	10	40	20
4	15	40	20

5	20	40	20
6	30	40	20
7	50	40	20
8	5	50	20
9	10	50	20
10	15	50	20
11	20	50	20
12	5	60	20
13	10	60	20
14	15	60	20
15	20	60	20
16	5	30	20
17	10	30	20
18	15	30	20
19	20	30	20

The selection of the investigated current density range was based on preliminary experiments. At current densities below approximately 5 mA cm^{-2}, nickel deposition proceeded slowly, resulting in relatively thin coatings after the fixed deposition time. Although these conditions may be useful for preparing ultrathin functional films, they are less suitable for practical catalyst fabrication where sufficient catalyst loading is required. Conversely, deposition at current densities above approximately 20 mA cm^{-2} substantially accelerated metal reduction but increased the probability of internal stress development and other process instabilities. Consequently, the intermediate current density interval was considered most relevant for the optimization of catalyst preparation.

Electrolyte temperature represents another critical process parameter because DESs exhibit significantly higher viscosities than aqueous electrolytes. Increasing temperature decreases viscosity while simultaneously enhancing ionic conductivity and diffusion coefficients of electroactive species. Faster transport of nickel ions toward the cathode reduces concentration polarization and facilitates more stable deposition, particularly at elevated current densities where mass transport limitations become increasingly significant.

Temperature additionally influences the electrochemical reduction kinetics by reducing charge-transfer resistance and increasing exchange current density. These combined effects decrease the cathodic overpotential required to sustain a given deposition current, thereby improving the energetic efficiency of the electrodeposition process. However, excessively high temperatures may accelerate electrolyte degradation or alter solvent composition through evaporation of absorbed moisture; therefore, optimization must balance electrochemical performance with electrolyte stability and long-term process reproducibility.

During all experiments, deposition potentials were continuously monitored under galvanostatic conditions until steady-state values were reached. Initially, transient potential changes associated with nickel nucleation and early crystal growth were observed. After approximately 10–15 min, the potential stabilized, indicating establishment of a quasi-steady deposition regime in which the rates of nickel-ion reduction, ionic transport, and crystal growth approached dynamic equilibrium. These stabilized potentials were subsequently used for constructing stationary current density–potential relationships and evaluating the influence of deposition parameters on electrochemical behaviour.

The systematic optimization performed in this study established an experimental window suitable for preparing nickel catalysts from Ethaline-based electrolytes with excellent reproducibility. The optimized deposition parameters subsequently served

as the basis for the preparation of Ni/MoS_2 composite coatings described in Section 1.5.

1.4.5 Influence of Temperature and Current Density

The electrochemical behaviour of nickel electrodeposition from Ethaline-based electrolytes is governed primarily by two experimentally controlled variables: applied current density and electrolyte temperature (Fig. 2). Both parameters directly influence the reduction kinetics of Ni^{2+} ions, the magnitude of cathodic polarization, ionic transport within the electrolyte, and the overall deposition rate. Understanding their combined influence is therefore essential for developing reliable synthesis protocols for advanced electrocatalytic materials.

The relationship between deposition current density and electrode potential was evaluated using stationary polarization curves constructed from chronopotentiometric measurements performed under galvanostatic conditions (Fig. 2). After stabilization of the electrode potential, steady-state values were extracted and plotted as a function of the applied current density. These stationary polarization curves provide valuable information regarding the electrochemical kinetics of nickel deposition in deep eutectic solvents and allow direct comparison of the influence of electrolyte temperature on the reduction process.

For all investigated temperatures, increasing current density resulted in progressively more negative deposition potentials. This behaviour is characteristic of electrochemical reduction processes operating under activation-controlled conditions, where larger cathodic overpotentials are required to sustain faster electron-transfer rates. Higher current densities increase the demand for nickel-ion reduction at the electrode surface, thereby increasing electrochemical polarization.

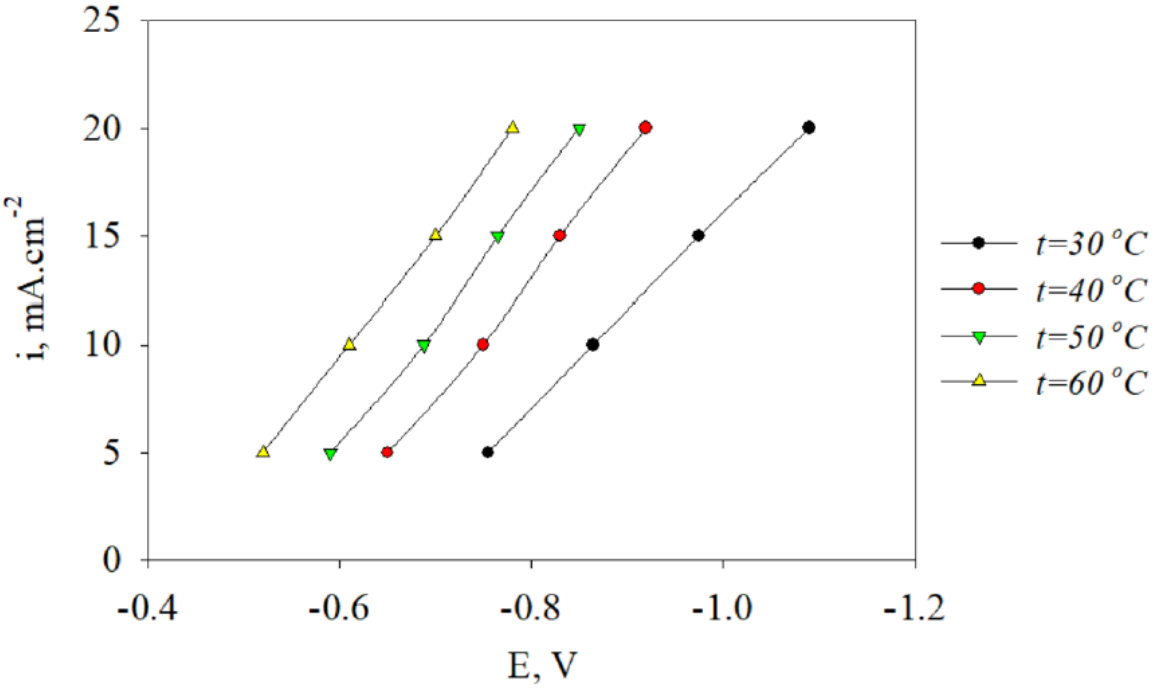


Figure 2. Stationary i-E curves of Ni electrodeposition from an Ethaline-based electrolyte constructed from steady-state potentials obtained during chronopotentiometric measurements.

A pronounced influence of electrolyte temperature was observed throughout the investigated current density range. Increasing the temperature from 30 to 60 °C systematically shifted the polarization curves toward less negative potentials, demonstrating that nickel reduction became electrochemically more favorable at elevated temperatures. This behaviour can be attributed to several mutually reinforcing effects associated with thermal activation.

Firstly, higher temperatures substantially reduce the viscosity of the Ethaline electrolyte, resulting in improved mobility of solvated nickel ions and enhanced ionic conductivity. Lower viscosity decreases resistance to ion transport, facilitating faster replenishment of nickel ions at the cathode surface and reducing concentration polarization during deposition.

Secondly, elevated temperature accelerates charge-transfer kinetics at the electrode/electrolyte interface by increasing the frequency of successful electron-transfer events. The activation energy associated with nickel reduction is therefore overcome more readily, allowing deposition to proceed at lower cathodic overpotentials.

Finally, higher temperatures improve diffusion within the electrolyte, reducing concentration gradients that develop adjacent to the electrode during galvanostatic deposition. The combined improvements in diffusion, migration, and electrochemical kinetics explain the systematic shift of the polarization curves toward lower polarization with increasing temperature.

These observations demonstrate that deposition temperature can be used as an effective process variable for controlling electrochemical performance without modifying electrolyte composition. Operation at elevated temperature permits higher deposition rates while maintaining lower cathodic polarization.

From a technological perspective, optimization of both temperature and current density is particularly important because these parameters also determine the practical productivity of electrodeposition. Increasing current density directly increases the amount of nickel deposited per unit time, whereas increasing temperature facilitates this higher deposition rate by improving ionic transport and reducing electrochemical losses. Consequently, the optimal synthesis conditions represent a compromise between maximizing deposition productivity and maintaining stable electrochemical behaviour.

The polarization studies performed during WP1 therefore established the electrochemical operating window used for subsequent preparation of advanced nickel-based catalysts and Ni/MoS_2 composite coatings. The optimized conditions provide sufficiently rapid deposition while minimizing unnecessary energy consumption associated with excessive cathodic polarization.

1.4.6 Current Efficiency of Ni Electrodeposition

Current efficiency represents one of the most important quantitative parameters for evaluating electrochemical deposition processes because it describes the fraction of supplied electrical charge that is effectively utilized for metal deposition. High current efficiency indicates that the majority of electrons contribute directly to nickel reduction, whereas lower efficiencies signify increasing contributions from competing side reactions, most notably hydrogen evolution.

The current efficiency of nickel electrodeposition was determined gravimetrically by comparing the experimentally measured mass increase of the cathode with the theoretical mass predicted by Faraday's law. The current efficiency was calculated according to:

$$CE=(m_{exp}/m_{theor})\times 100\%,$$

where m_{exp} represents the experimentally measured mass of deposited nickel and m_{theor} corresponds to the theoretical mass calculated from the total electric charge passed during deposition according to Faraday's law. The theoretical deposited mass was determined using

$$m_{theor}=(M\ I\ \tau)/(nF),$$

where M is the molar mass of nickel, I is the applied current, τ is the deposition time, n = 2 is the number of electrons involved in the reduction of Ni^{2+} ions, and F is the Faraday constant.

The calculated current efficiencies demonstrated excellent electrochemical performance throughout the investigated deposition window (Fig. 3). Under all experimental conditions, current efficiency remained between approximately **97.6 and 100%**, indicating nearly complete utilization of the supplied electrical charge for nickel deposition. Such high efficiencies are particularly noteworthy

considering that electrodeposition was performed over a relatively broad range of current densities and temperatures.

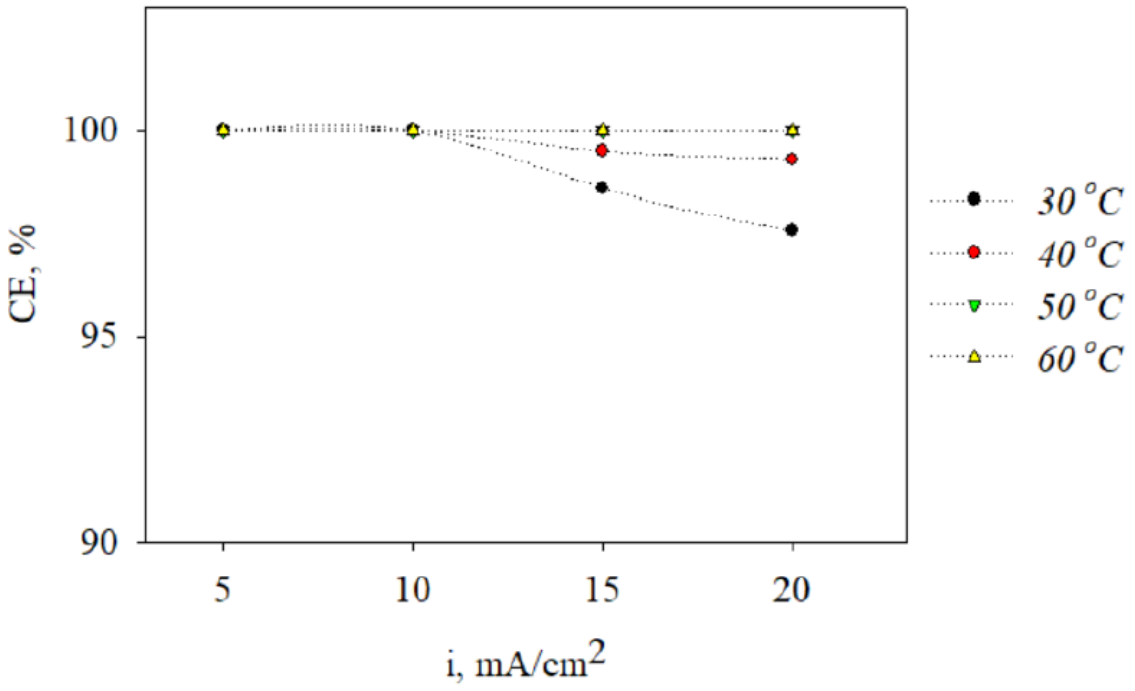


Figure 3. Effect of temperature and current density on current efficiency of Ni electrodeposition in the Ethaline-based electrolyte.

The slightly lower efficiencies observed at 30 °C are attributed primarily to the higher viscosity of the deep eutectic solvent at lower temperatures. Reduced ionic mobility limits mass transport of nickel ions toward the electrode surface and may promote minor contributions from competing electrochemical processes. Nevertheless, even under these conditions the current efficiency remained close to 98%, confirming the excellent suitability of the Ethaline electrolyte for nickel electrodeposition.

As the electrolyte temperature increased, the current efficiency approached 100% across the investigated current density range. Improved ionic conductivity and faster

diffusion substantially enhanced nickel-ion transport while simultaneously suppressing concentration polarization. Consequently, almost all supplied electrical charge was converted directly into metallic nickel.

The exceptionally high current efficiencies obtained during this study represent one of the principal advantages of deep eutectic solvent electrolytes over conventional aqueous plating baths. In aqueous systems, hydrogen evolution frequently competes with nickel deposition at elevated cathodic overpotentials, reducing Faradaic efficiency and increasing energy consumption. In contrast, the wider electrochemical stability window of Ethaline effectively suppresses parasitic hydrogen evolution, enabling highly efficient utilization of electrical energy for metal deposition.

From the perspective of catalyst manufacturing, these results demonstrate that DES-based nickel electrodeposition is not only environmentally attractive but also highly efficient in terms of energy utilization and raw material conversion. High current efficiency minimizes electricity consumption, reduces material losses, improves process reproducibility, and facilitates accurate prediction of deposited catalyst loading based solely on the applied electric charge. Such characteristics are particularly advantageous for future scale-up of catalyst production and industrial implementation of sustainable electrodeposition technologies.

1.4.7 Deposition Rate

In addition to current efficiency, the deposition rate represents an important technological parameter governing the practical applicability of an electrodeposition process. For catalyst preparation, an appropriate deposition rate is essential because it determines the amount of catalytically active material deposited per unit time and directly influences manufacturing productivity. Furthermore, the deposition rate

provides valuable information regarding the kinetics of metal reduction and the efficiency of mass transport within the electrolyte.

The average deposition rate of nickel was determined gravimetrically from the measured mass increase of the cathode after electrodeposition and expressed as the deposited mass per unit area and unit time. Assuming uniform deposition over the exposed electrode surface, the deposition rate was calculated according to

$$DR = m_{exp}/\rho A\,\tau,$$

where DR is the deposition rate, m_{exp} is the mass of deposited nickel in g, ρ is the density of nickel (8.90 $g \cdot cm^{-3}$), A is the geometric surface area of the working electrode in cm^2, and τ is the deposition time in min.

The obtained results (Fig. 4) demonstrated that the deposition rate increased almost linearly with increasing applied current density throughout the investigated operating range. This behaviour is consistent with Faraday's law, which predicts that the deposited metal mass is directly proportional to the total electric charge passed through the electrochemical cell. Because the current efficiency remained close to 100% under nearly all investigated conditions, almost the entire electrical charge contributed to nickel reduction, resulting in a nearly proportional relationship between applied current density and deposition rate.

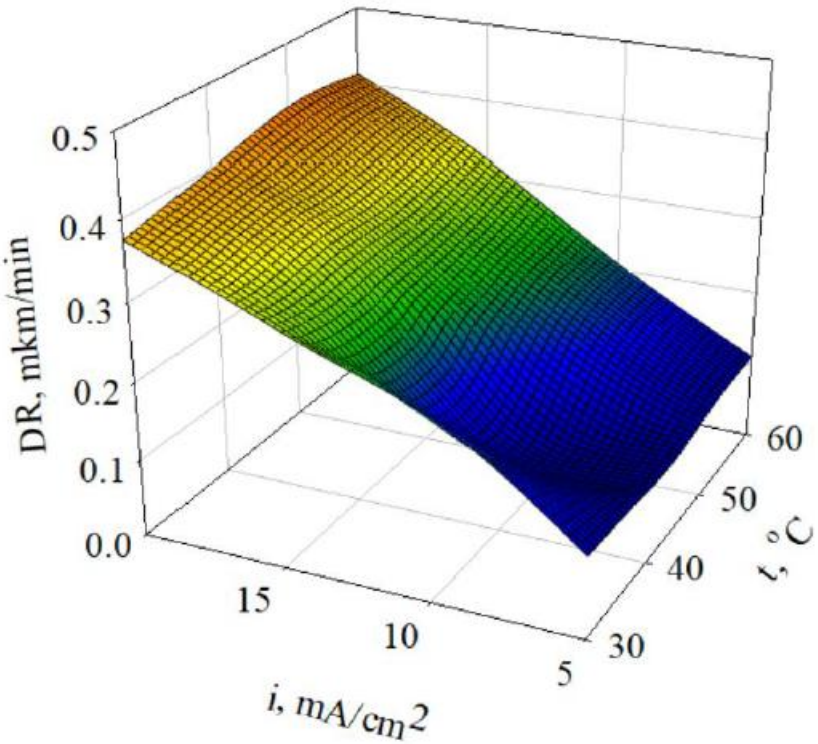


Figure 4. 3D plot illustrating the influence of deposition current density and electrolyte temperature on deposition rate of Ni in Ethaline-based electrolyte.

Electrolyte temperature also had a measurable influence on deposition productivity (Fig. 4). Increasing the temperature from 30 to 60 °C enhanced the deposition rate for all investigated current densities. This improvement can be attributed primarily to the reduction in electrolyte viscosity and the corresponding increase in ionic conductivity and diffusion coefficients. Enhanced transport of Ni^{2+} ions toward the cathode minimizes concentration polarization and allows higher rates of electrochemical reduction without significant depletion of electroactive species at the electrode surface.

The influence of temperature became increasingly significant at higher current densities, where diffusion limitations are generally more pronounced. Under these conditions, elevated temperature effectively compensates for the increased demand

for nickel ions by accelerating mass transport within the electrolyte. Consequently, stable deposition could be maintained even at relatively high current densities without evidence of severe transport limitations.

From a technological perspective, the observed behaviour demonstrates that deposition productivity may be controlled through simultaneous adjustment of current density and electrolyte temperature. While increasing current density directly increases the amount of deposited nickel per unit time, higher operating temperatures improve the efficiency of this process by reducing electrochemical polarization and facilitating rapid ion transport. The combination of these effects enables efficient catalyst preparation without compromising the excellent current efficiencies characteristic of the Ethaline-based electrolyte.

The high deposition rates achieved under optimized conditions are particularly advantageous for future scale-up of catalyst production. The nearly quantitative conversion of electrical energy into deposited nickel minimizes energy losses and shortens processing times, making DES-based electrodeposition an attractive alternative to conventional aqueous plating technologies for manufacturing nickel-based electrocatalysts.

1.4.8 Selection of Optimal Conditions for Subsequent Ni/MoS_2 Composite Electrodeposition

The optimization of pure Ni electrodeposition established a broad operating range in which Ni^{2+} reduction proceeded with high current efficiency and reproducible electrochemical behaviour. However, the conditions favorable for deposition of pure Ni cannot be transferred directly to the electrodeposition of Ni/MoS_2 composite coatings. Composite electrodeposition introduces an additional requirement: the MoS_2 particles must remain sufficiently dispersed in the electrolyte and available near the cathode surface throughout the deposition process.

The incorporation of solid particles into an electrodeposited metal matrix generally involves several consecutive stages. Suspended particles are transported through the bulk electrolyte toward the cathode, become weakly adsorbed at the electrode–electrolyte interface, and are subsequently captured by the growing Ni layer. The amount of MoS_2 incorporated into the composite therefore depends not only on the electrochemical reduction rate of nickel ions but also on the stability of the colloidal electrolyte and the local particle concentration near the working electrode.

Ethaline-based electrolytes are advantageous for composite electrodeposition because their relatively high viscosity can slow gravitational settling and help maintain suspended particles in the electrolyte. This characteristic is particularly important when electrodeposition is conducted without continuous mechanical stirring. Under static conditions, the stability of the colloidal suspension becomes a decisive process parameter because sedimentation progressively depletes particles from the upper and central regions of the electrochemical cell.

Although increasing temperature improves the conductivity of the DES-based electrolyte and accelerates nickel-ion transport, it simultaneously decreases the viscosity of the liquid phase. For pure Ni deposition, this reduction in viscosity is generally beneficial because it decreases mass-transfer resistance and cathodic polarization. For Ni/MoS_2 composite electrodeposition, however, lower viscosity may have an adverse effect by increasing the sedimentation velocity of MoS_2 particles.

Accelerated sedimentation reduces the concentration of dispersed particles in the vicinity of the cathode. Consequently, fewer particles reach and adsorb on the electrode surface before being captured by the growing nickel matrix. The resulting composite may therefore contain a lower MoS_2 loading than coatings prepared from a more viscous and stable suspension. Since MoS_2 supplies catalytically active sites

for the hydrogen evolution reaction, insufficient particle incorporation can reduce the catalytic benefit expected from formation of the Ni/MoS_2 composite.

The influence of temperature on composite deposition must therefore be considered as a balance between two opposing effects:

- increasing temperature improves ionic conductivity and accelerates Ni^{2+} reduction;
- increasing temperature decreases electrolyte viscosity, accelerates MoS_2 sedimentation, and may reduce particle availability near the cathode.

In the absence of electrolyte stirring, the second effect may become dominant. Consequently, the highest temperatures investigated for pure nickel deposition should not automatically be regarded as optimal for Ni/MoS_2 composite preparation. A moderate deposition temperature is more appropriate because it maintains sufficient ionic conductivity for nickel deposition while retaining enough viscosity to limit rapid particle settling.

Current density must also be selected carefully. At very low current densities, nickel matrix formation proceeds slowly and catalyst preparation becomes inefficient. At excessively high current densities, the nickel layer grows rapidly, potentially reducing the relative amount of MoS_2 incorporated into the deposit. Rapid matrix growth may also capture particles non-uniformly if the local particle supply cannot keep pace with nickel deposition.

For subsequent Ni/MoS_2 composite electrodeposition, an intermediate current density should therefore be combined with a moderate electrolyte temperature. Based on the operating window established for pure nickel deposition, a current density of approximately 10–15 mA cm^{-2} remains suitable. However, the temperature should be selected closer to 40 °C, rather than the upper range of 50–60 °C, particularly when deposition is carried out from an unstirred colloidal electrolyte.

At approximately 40 °C, the Ethaline-based electrolyte provides sufficient conductivity and nickel-ion mobility for stable electrodeposition while retaining comparatively high viscosity. This compromise is expected to decrease the rate of MoS_2 sedimentation, maintain a more uniform particle concentration near the cathode, and promote greater incorporation of MoS_2 into the growing nickel matrix. The duration between preparation of the colloidal electrolyte and the beginning of electrodeposition should also be minimized. Following dispersion of MoS_2, the electrolyte should be transferred promptly to the electrochemical cell and the deposition procedure initiated without unnecessary delay. The position and orientation of the working electrode should remain consistent between experiments because particle sedimentation can produce vertical concentration gradients within an unstirred cell.

Accordingly, the preliminary conditions selected for subsequent Ni/MoS_2 composite electrodeposition were:

- an intermediate current density of approximately 10–15 mA cm^{-2};
- a moderate electrolyte temperature of approximately 40 °C;
- a fixed deposition time selected to provide sufficient catalyst loading;
- freshly dispersed MoS_2-containing electrolyte;
- minimized delay between particle dispersion and electrodeposition;
- consistent electrode position and cell geometry;
- avoidance of elevated temperatures that would excessively reduce viscosity and accelerate sedimentation.

These conditions represent a compromise between efficient nickel matrix deposition and preservation of colloidal stability. Final optimization of the composite process must consider MoS_2 concentration in the electrolyte, sedimentation behaviour, particle incorporation efficiency, deposition duration, and the possible use of controlled agitation or recirculation.

1.4.9 Summary

Ni electrodeposition from the Ethaline-based solvent was successfully established as the primary synthesis route for the preparation of nickel electrocatalysts within WP 1. The systematic investigation of deposition parameters demonstrated that the DES electrolyte provides a stable and highly efficient medium for electrochemical nickel deposition while overcoming several limitations associated with conventional aqueous plating baths.

Optimization of the electrodeposition process revealed that both applied current density and electrolyte temperature significantly influence deposition kinetics. Increasing current density accelerated nickel deposition, whereas increasing electrolyte temperature reduced cathodic polarization through improved ionic conductivity, enhanced diffusion of nickel ions, and reduced electrolyte viscosity. These combined effects facilitated efficient electrodeposition over a broad operating window.

Gravimetric evaluation showed exceptionally high current efficiencies ranging from approximately 97.6 to 100%, confirming that nearly all supplied electrical charge contributed directly to nickel reduction. The suppression of competing hydrogen evolution, enabled by the wide electrochemical stability window of the deep eutectic solvent, represents one of the principal advantages of the DES-based deposition process and contributes to its high energy efficiency.

Considering deposition kinetics, current efficiency, and process reproducibility, the study established a broad operating window for pure nickel electrodeposition. Intermediate current densities of approximately 10–15 mA cm^{-2} provided an appropriate balance between deposition productivity and process control. Elevated temperatures improved pure nickel deposition by reducing electrolyte viscosity and cathodic polarization.

However, the conditions favorable for pure nickel deposition are not necessarily optimal for Ni/MoS_2 composite electrodeposition. In an unstirred colloidal electrolyte, increasing temperature decreases viscosity and accelerates particle sedimentation, thereby lowering the MoS_2 concentration near the cathode and reducing particle incorporation into the nickel matrix. For subsequent composite deposition, a moderate temperature of approximately 40 °C was therefore selected as a more suitable compromise between nickel-ion transport and colloidal stability. Maintaining sufficient MoS_2 availability near the electrode is essential because reduced particle incorporation may lead directly to lower catalytic activity of the resulting composite coating.

1.5 Electrodeposition of Ni/MoS_2 composite coatings for catalytic HER

1.5.1 Preparation of a colloidal Ethaline-based electrolyte for the electrodeposition of MoS_2-containing Ni composites

The preparation of a colloidal electrolyte for MoS_2/Ni composite coating electrodeposition can be realized using three possible strategies.

The first approach involves the *in-situ* synthesis of MoS_2 nanoparticles directly within the electrolyte used for Ni electrodeposition. This method ensures a high degree of dispersion and intimate interaction between MoS_2 and the electrolyte components, which may improve particle incorporation and adhesion to the Ni matrix. However, controlling the size, stoichiometry, and stability of the in situ–formed nanoparticles can be challenging, and side reactions may alter the electrolyte composition or affect the nickel deposition process.

The second approach is to synthesize MoS_2 nanoparticles separately in an Ethaline medium, followed by isolation, purification, and re-dispersion into the Ni electrodeposition bath. This method allows better control over particle size, crystallinity, and surface chemistry before incorporation. Nevertheless, the

additional synthesis and separation steps make this route more complex and time-consuming, and re-dispersion of MoS_2 particles without aggregation can be difficult.

The third and most practical approach is the use of commercially available MoS_2 nanopowders, which can be directly dispersed into the Ni electrolyte to form a colloidal suspension. This method is straightforward, reproducible, and suitable for scale-up. However, ensuring uniform and stable dispersion of the particles in the viscous Ethaline-based electrolyte may require optimization of surfactant concentration, stirring rate, or ultrasonic treatment to prevent sedimentation and agglomeration.

1.5.1.1 Synthesis of MoS_2 in Ethaline-based electrolytes

To prepare colloidal dispersions of MoS_2 nanoparticles for Ni–MoS_2 composite electrodeposition, several synthesis routes were explored using an Ethaline-based deep eutectic solvent (DES) as the reaction medium. The syntheses were conducted according to different precursor concentrations, reducing agent ratios, and solvent compositions, as summarized in samples MOS-1 to MOS-10.

In all experiments, ammonium tetrathiomolybdate ($(NH_4)_2MoS_4$) served as the molybdenum precursor, while L-ascorbic acid acted as a mild reducing agent promoting the conversion of Mo(VI) to Mo(IV) and subsequent formation of MoS_2. Ethaline (a 1:2 molar mixture of choline chloride and ethylene glycol) was used either in its pure form or in combination with deionized water to form a mixed solvent system (DES:H_2O = 3:1, v/v). The reaction temperature was maintained at 65 °C, providing sufficient thermal energy to drive reduction and sulfide formation under mild conditions.

The general procedure involved dissolving a weighed amount of $(NH_4)_2MoS_4$ in 40 mL of DES (or in 30 mL DES + 10 mL water for mixed systems). The solution was stirred for 1 hour at 65 °C until complete dissolution of the precursor.

Subsequently, the required amount of L-ascorbic acid was added under continuous stirring. The reaction mixture was then maintained at 65 °C for an additional 2 hours, during which the color of the solution gradually changed from orange-red to dark brown or black, indicating the formation of colloidal MoS_2.

Different synthesis routes (MOS-1 – MOS-10) varied in the precursor concentration, L-ascorbic acid amount, and solvent composition, as outlined below:

- ***Effect of Reducing Agent Amount:***

In MOS-1 and MOS-2 (using 3.124 mmol of $(NH_4)_2MoS_4$ in 40 mL DES), the L-ascorbic acid amount was varied from equimolar (3.124 mmol) to double molar ratio (6.248 mmol). Similarly, in MOS-5 and MOS-6 (lower precursor concentration, same solvent), and MOS-3/MOS-4 (DES–water mixture), the same molar ratios were applied. A higher L-ascorbic acid amount resulted in a faster color change and denser colloid formation, indicating more efficient reduction and nucleation of MoS_2 particles.

- ***Effect of Solvent Composition:***

In samples MOS-3, MOS-4, MOS-7, and MOS-8, partial replacement of DES with water reduced the viscosity of the medium, improving mass transport and promoting more uniform particle formation. However, excessive water content may affect DES stability and particle dispersion.

- ***Effect of Precursor Concentration:***

Higher precursor concentration (MOS-1, MOS-2, MOS-7, MOS-8) led to more concentrated colloidal dispersions with stronger coloration, while lower concentrations (MOS-3 – MOS-6, MOS-9, MOS-10) produced lighter suspensions with potentially smaller and more dispersed particles.

In all cases, visual observation of the color change confirmed successful reduction and formation of MoS_2 nanoparticles within the Ethaline-based medium.

The obtained MoS_2-containing extracts were used as additive components for preparing composite electrolytes for Ni–MoS_2 electrodeposition. A base Ethaline-based nickel electrolyte was first prepared by dissolving the required amounts of nickel(II) chloride hexahydrate ($NiCl_2 \cdot 6H_2O$) as the Ni source and boric acid (H_3BO_3) as the buffering agent in Ethaline, followed by the addition of a small, controlled amount of deionized water to adjust conductivity and viscosity.

The MoS_2-containing extracts obtained from synthesis steps indicated above were then thoroughly mixed with this base Ni electrolyte to achieve the final electrolyte compositions specified in Table 1, additionally containing MoS_2 particles in a concentration of 5 $g \cdot L^{-1}$. The prepared mixtures were continuously stirred and ultrasonicated to ensure uniform dispersion of the MoS_2 nanoparticles and to prevent sedimentation before electrodeposition.

These prepared composite electrolytes were subsequently used to electrodeposit Ni–MoS_2 composite coatings, incorporating catalytically active MoS_2 particles into the Ni matrix to enhance hydrogen evolution reaction performance.

1.5.1.2 Synthesis, isolation, and re-dispersion of MoS_2 nanoparticles in Ethaline-based electrolyte for Ni/MoS_2 composite electrodeposition

An alternative approach for preparing Ni–MoS_2 composite electrolytes involves the separate synthesis of MoS_2 nanoparticles in an Ethaline-based medium, followed by their isolation, purification, and re-dispersion into the Ni electrodeposition bath. This route allows precise control over the structural and chemical properties of MoS_2 before its incorporation into the Ni matrix.

Synthesis of MoS_2 Nanoparticles in Ethaline:

The synthesis can be carried out using ammonium tetrathiomolybdate ($(NH_4)_2MoS_4$) as the Mo precursor and L-ascorbic acid as a mild reducing agent.

Typically, a known amount of $(NH_4)_2MoS_4$ is dissolved in Ethaline under magnetic stirring at 65–80 °C until complete dissolution. Subsequently, L-ascorbic

acid is added in equimolar or slightly excess ratio relative to the precursor to initiate the reduction of Mo(VI) to Mo(IV) and the formation of MoS_2 nanoparticles according to the reaction:

$$(NH_4)_2MoS_4 + \text{reducing agent} \rightarrow MoS_2 + S + \text{byproducts}.$$

The reaction mixture is maintained under stirring for several hours until the color changes from orange-red to dark brown or black, indicating MoS_2 formation. The resulting colloidal suspension typically contains uniformly distributed MoS_2 nanoparticles stabilized by weak interactions with the Ethaline components (choline chloride and ethylene glycol).

Isolation and Purification:

After synthesis, the MoS_2 nanoparticles are separated from the reaction medium by centrifugation (e.g., 8000–10,000 rpm for 10–15 min). The solid product is then washed several times with ethanol and deionized water to remove unreacted precursors, organic residues, and excess Ethaline components. Finally, the purified MoS_2 powder is dried under vacuum or mild heating (50–60 °C) until constant weight is achieved.

This step yields a clean MoS_2 nanopowder with minimal surface contamination, suitable for re-dispersion in electroplating baths.

Re-Dispersion into Ni Electrodeposition Bath:

The purified MoS_2 nanoparticles are re-dispersed in the Ethaline-based Ni electrolyte, which contains nickel(II) chloride hexahydrate ($NiCl_2 \cdot 6H_2O$) as the metal source and boric acid (H_3BO_3) as a buffer component. To achieve a uniform dispersion and prevent agglomeration, the MoS_2 powder is first ultrasonicated in a small amount of Ethaline or a water–Ethaline mixture for 30–60 minutes. The resulting suspension is then added to the Ni electrolyte under continuous stirring to obtain the final composite bath with a MoS_2 concentration of approximately 5 $g \cdot L^{-1}$ (other components as specified in Table 1).

Proper dispersion of MoS_2 is critical to ensure homogeneous incorporation of nanoparticles into the Ni matrix during electrodeposition. Ultrasonic agitation and mechanical stirring before deposition help maintain colloidal stability.

Advantages and Considerations:

This synthesis route offers several advantages, including precise control over particle size, crystallinity, and purity, as well as the possibility to modify surface chemistry through post-synthesis treatments. However, it is more labor-intensive and involves additional steps such as separation, washing, and re-dispersion. Moreover, care must be taken to maintain particle stability and prevent aggregation upon introduction into the viscous Ethaline-based Ni electrolyte.

Thus, this proposed method provides a versatile and tunable pathway for producing well-defined MoS_2 nanoparticles suitable for controlled incorporation into Ni composite coatings for enhanced HER catalytic performance.

1.5.1.3 Preparation of Ni–MoS_2 containing electrolyte using commercial MoS_2 powder

To prepare the electrolyte for Ni–MoS_2 composite electrodeposition, commercial MoS_2 nanopowder (Japan origin, average particle size ≈ 90 nm) was utilized as the source of catalytic nanoparticles. This approach allows for straightforward preparation, good reproducibility, and controlled addition of MoS_2 into the Ni electrolyte without requiring in-situ synthesis or chemical reduction steps.

Electrolyte Composition and Preparation Procedure:

A total of 200 ml of composite electrolyte was prepared with the composition presented in table 3.

The preparation was carried out as follows:

1. ***Base electrolyte preparation:*** The required amounts of $NiCl_2 \cdot 6H_2O$ and boric acid were dissolved in a mixture of Ethaline and deionized water (30 wt.% water) under constant stirring at 60 °C until complete dissolution. This produced a

homogeneous Ni-based plating solution with appropriate conductivity and buffering capacity.

2. ***Addition of MoS_2 nanoparticles:*** The commercial MoS_2 nanopowder was gradually added to the base electrolyte to achieve a final concentration of 1 g L^{-1}. To ensure uniform dispersion and to minimize particle agglomeration, the suspension was ultrasonicated for 30 minutes and subsequently stirred magnetically for an additional hour at 50–60 °C.

3. ***Stabilization:*** Before electrodeposition, the prepared composite electrolyte was kept under gentle stirring to maintain a stable colloidal suspension and uniform particle distribution.

Table 3. Formulation and component concentrations of the Ni–MoS_2 composite electrolyte.

Component	**Content**
$NiCl_2 \cdot 6H_2O$	1.0 M
H_3BO_3 (Boric acid)	0.13 M
Additional water	30 wt.%
Ethaline (choline chloride + ethylene glycol, 1:2 molar ratio)	balance
MoS_2 nanopowder	1 g L^{-1}

The use of commercial MoS_2 nanoparticles simplifies the electrolyte preparation process, avoiding multiple synthesis or purification steps. The small particle size (≈ 90 nm) ensures a large active surface area and promotes uniform incorporation into the Ni matrix during electrodeposition. However, due to the relatively high

viscosity of Ethaline and the hydrophobic nature of MoS_2, proper dispersion control via ultrasonication and continuous stirring is essential to prevent sedimentation and achieve reproducible coating morphology.

It should be noted that the resulting Ni–MoS_2 composite electrolyte was stable, homogeneous, and prepared for subsequent electrodeposition experiments aimed at creating catalytic coatings with improved HER activity.

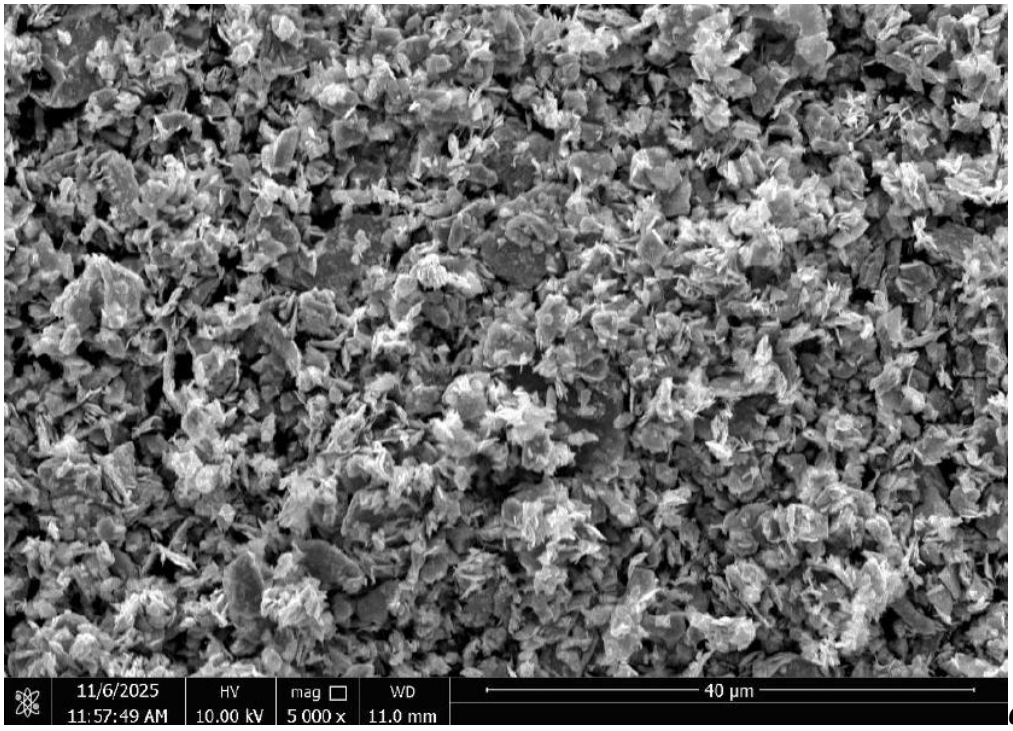
1.5.1.4 Comparison of commercial and synthesized MoS_2 powders

Before depositing Ni/MoS_2 composite coatings, it was necessary to compare the commercial MoS_2 powder with those synthesized in Ethaline. The chemical composition, crystallinity, and particle size and shape can significantly impact how MoS_2 particles are incorporated into the Ni matrix. Additionally, these factors may influence the growth characteristics of the Ni matrix itself. Therefore, the dried MoS_2 powders were analyzed using SEM and EDX. Figures 5 and 6 show the morphology, structure, and elemental composition of the examined powders.

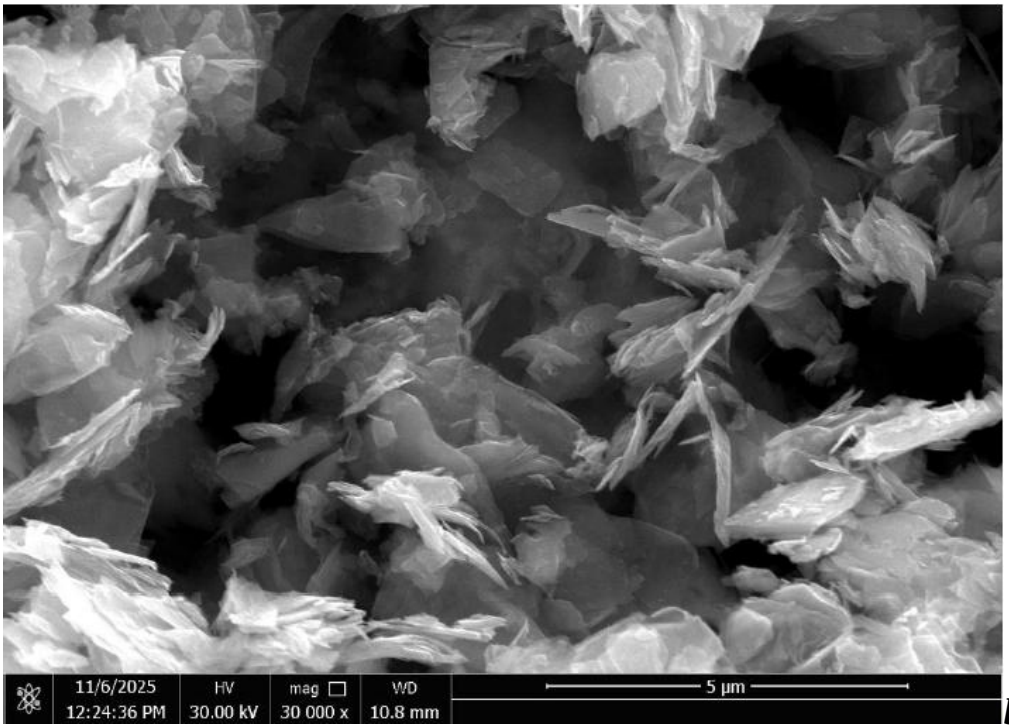
SEM images of the commercial MoS_2 powder at different magnifications are shown in Fig. 5a and 5b. The corresponding EDX spectrum is presented in Fig. 5c. The EDX analysis revealed the presence of small amounts of oxygen and carbon. The detected carbon signal most likely originated from the carbon tape used to mount the powder particles, rather than from the powder itself. The minor oxygen signal can be attributed to slight surface oxidation of MoS_2 or to adsorbed oxygen-containing species resulting from exposure to air.

As shown in Fig. 6a and 6b, the MoS_2 powder synthesized in Ethaline displays a morphology significantly different from that of the commercial MoS_2 powder. The data clearly indicate that the synthesized powder mainly consists of much smaller, nanosized particles. It is important to note that the elemental composition of the synthesized powder (Fig. 6c) is similar to that of the commercial product. The

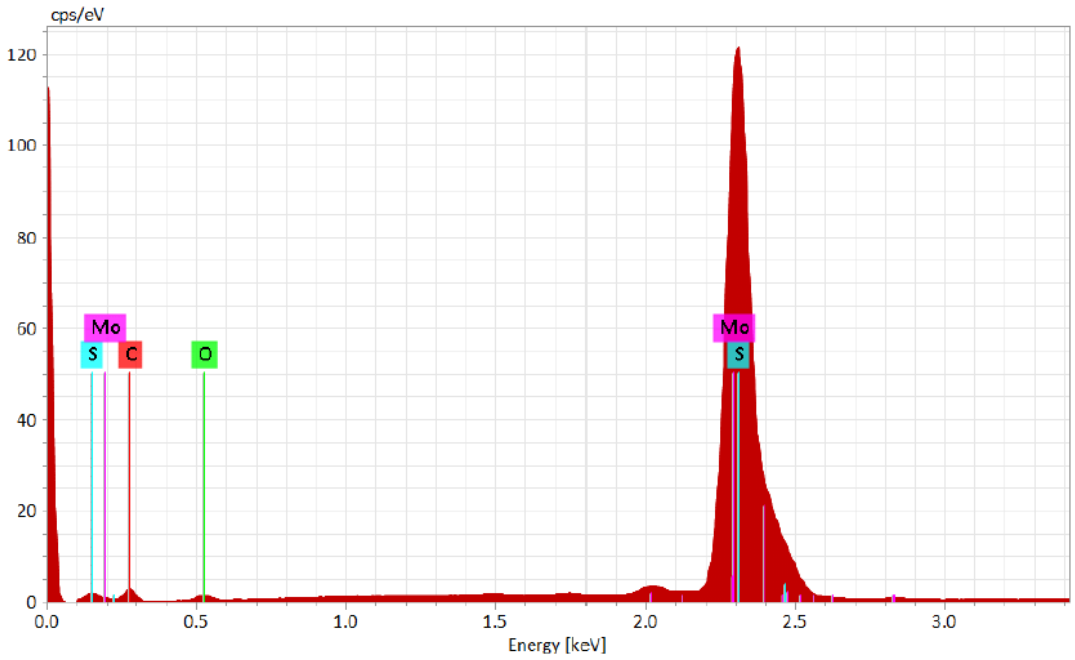
smaller nanosized particles of the synthesized MoS_2 powder have great potential as a catalytic component and may offer higher efficiency for HER compared with commercially available MoS_2 particles.



a

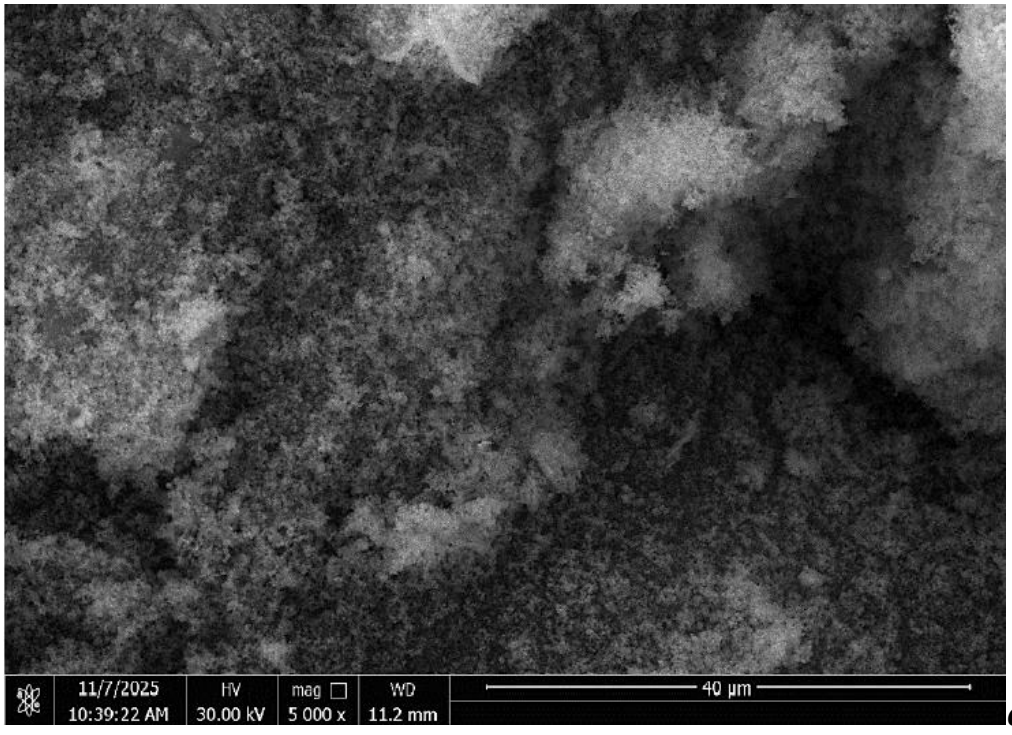


b

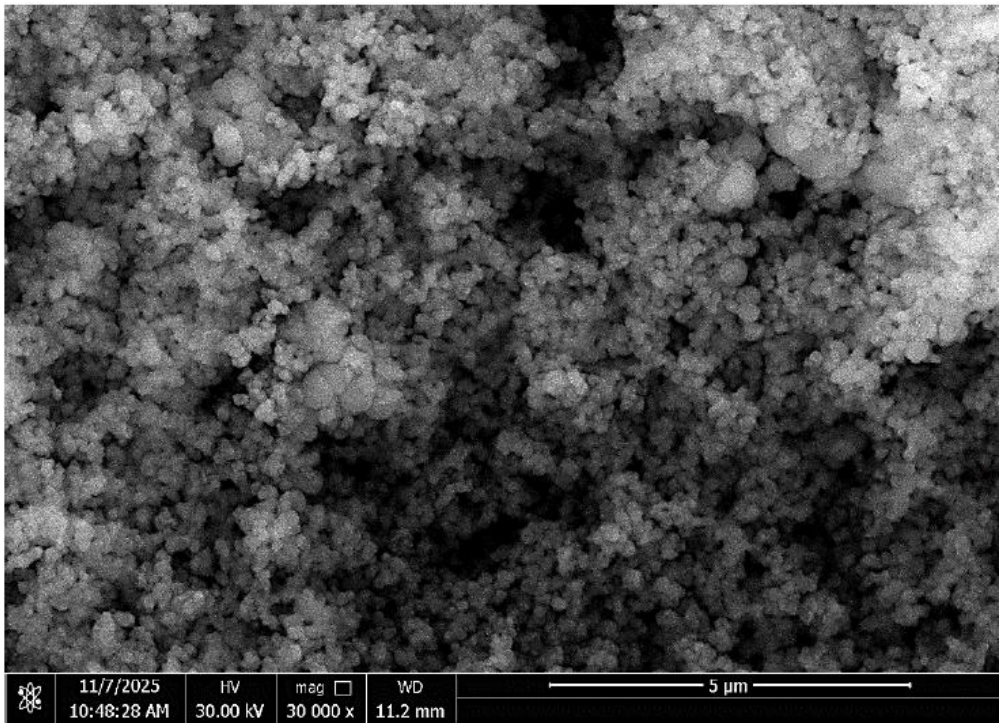


c

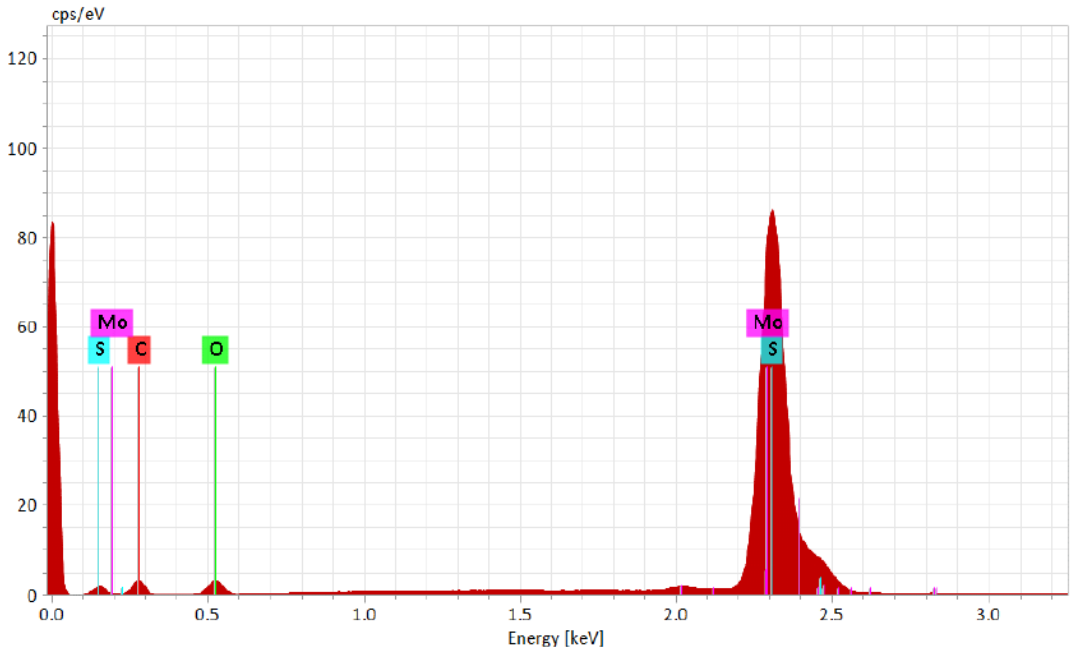
Figure 5. SEM images (a, b) and EDX spectrum (c) of the commercial MoS_2 powder. (a) Magnification: 5k, scale bar: 40 µm; (b) Magnification: 30k, scale bar: 5 µm.



a



b



c

Figure 6. SEM images (a, b) and EDX spectrum (c) of the synthesized in Ethaline MoS_2 powder. (a) Magnification: 5k, scale bar: 40 µm; (b) Magnification: 30k, scale bar: 5 µm.

1.5.2 Electrodeposition conditions for obtaining Ni/MoS_2 composite coatings from the Ethaline-based electrolyte: influence of different factors

The electrolyte composition used for the electrodeposition of Ni/MoS_2 composite coatings is presented in Table 3, while the electrodeposition conditions are summarized in Table 4.

Stationary i–E curves for Ni and Ni/MoS_2 electrodeposition from the Ethaline-based electrolyte were derived from the steady-state potentials measured during chronopotentiometric experiments and are shown in Figure 7. Figure 8 compares the deposition rates of Ni and Ni/MoS_2 coatings at different current densities. As seen, both datasets exhibit nearly identical behavior for Ni and Ni/MoS_2, indicating that adding MoS_2 does not significantly affect the kinetics of the electrodeposition process.

Table 4. Electrodeposition conditions for Ni/MoS_2 composite coatings.

Sample	i, mA/cm2	t, °C	τ, min
1	5	40	20
2	10		
3	15		
4	20		
5	25		

In light of this, it becomes particularly interesting to investigate whether the incorporation of MoS_2 influences the morphological features of the resulting coatings. Therefore, a detailed SEM analysis was carried out to examine the surface morphology.

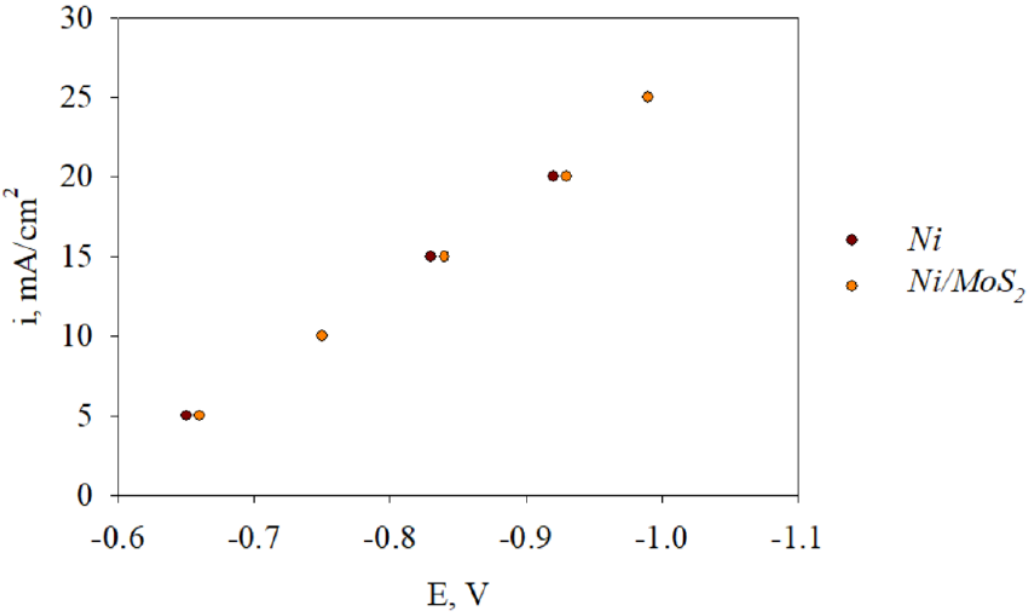


Figure 7. Stationary i-E curves of Ni and Ni/MoS_2 electrodeposition from an Ethaline-based electrolyte constructed from steady-state potentials obtained during chronopotentiometric measurements (t = 40 °C).

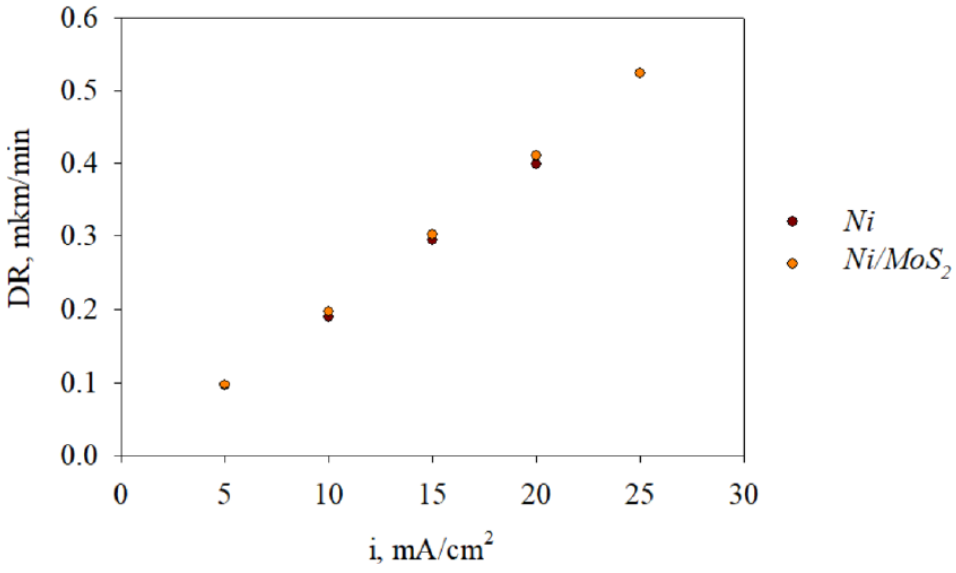


Figure 8. Influence of deposition current density on deposition rate of Ni and Ni/MoS_2 coatings in Ethaline-based electrolyte (t = 40 °C).

1.6 Thermal engineering of MoFeNiP carbon electrocatalysts for efficient hydrogen evolution in acidic and alkaline media

Transition metal phosphide (TMP)-based carbon electrocatalysts have emerged as one of the most promising alternatives to noble-metal catalysts for the HER because of their high intrinsic activity, excellent electrical conductivity, and favorable cost-effectiveness. Among them, multimetallic phosphides incorporating Mo, Fe, and Ni exhibit synergistic electronic interactions that optimize the hydrogen adsorption free energy, increase the density of catalytically active sites, and enhance structural stability under both acidic and alkaline conditions.

Thermal engineering provides an effective strategy to precisely regulate the crystallinity, phase composition, defect density, and metal–phosphorus coordination while simultaneously promoting strong coupling between the phosphide nanoparticles and conductive carbon matrices. Such structural optimization accelerates charge transfer, improves mass transport, and suppresses catalyst degradation during prolonged electrolysis. Consequently, thermally engineered MoFeNiP/carbon composites represent a highly attractive class of bifunctional HER electrocatalysts, offering excellent catalytic performance, long-term durability, and significant potential for scalable green hydrogen production in a wide range of water electrolysis technologies. Their compositional tunability and compatibility with sustainable synthesis routes further position these catalysts as promising candidates for next-generation renewable energy conversion and storage systems.

Catalyst synthesis:

To investigate the influence of thermal treatment on catalyst structure and HER performance, a series of MoFeNiP/carbon composites was synthesized using a polymer-derived approach. A homogeneous polyacrylonitrile (PAN)-based gel containing molybdenum, iron, and nickel chloride precursors together with phosphoric acid (H_3PO_4) was prepared in dimethylformamide (DMF). Following

solvent evaporation, the precursor underwent a multistep thermal treatment consisting of: (i) stabilization in air at 270 °C to crosslink the PAN matrix; (ii) pyrolysis under flowing Ar at 800, 1000, or 1200 °C to carbonize the polymer and promote the formation of metal-containing intermediate phases; and (iii) a final reduction/phosphidation treatment under an Ar/H_2 atmosphere at 780 °C to produce multimetallic MoFeNiP phosphides uniformly dispersed within the conductive carbon matrix. The resulting catalysts are denoted C-MoFeNiP-800, C-MoFeNiP-1000, and C-MoFeNiP-1200, according to their respective pyrolysis temperatures (Fig. 9).

This synthesis strategy enables systematic evaluation of the role of pyrolysis temperature on the phase composition, morphology, graphitization degree, and electrocatalytic HER performance of the resulting MoFeNiP/carbon composites, providing valuable insights into the relationship between thermal engineering, catalyst structure, and hydrogen evolution activity under both acidic and alkaline conditions.

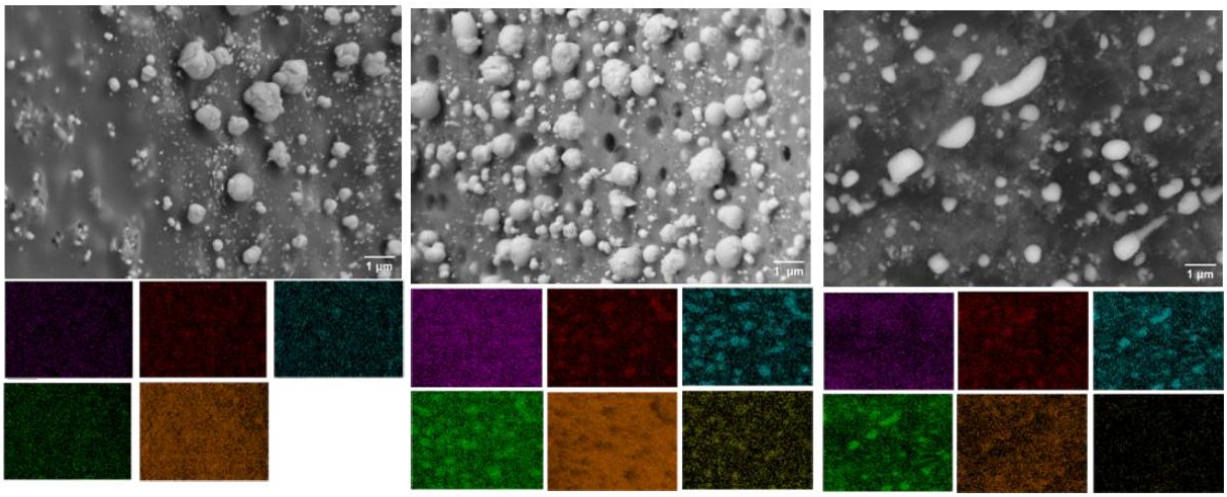


Figure 9. SEM images and corresponding mappings for (a) MoFeNiP-800, (b) Mo-FeNiP-1000, and (c) MoFeNiP-1200. Elemental distributions are color-

labeled as Mo (purple), Fe (red), Ni (blue), P (green), C (orange), and O (yellow). The elemental mapping images correspond to the SEM micrographs shown above (scale bar as indicated).

1.7 Preparation of catalytically active Ni foams by the replication method

The replication (template-assisted) method was employed to fabricate highly porous three-dimensional nickel foams with interconnected open-cell architecture. This approach is based on the impregnation of a sacrificial polymer template with a metal-containing slurry, followed by thermal removal of the polymer and subsequent sintering of the metallic phase. The resulting metallic foams possess high porosity, low density, and a large specific surface area, making them attractive as self-supported electrocatalysts and catalyst supports for electrochemical energy conversion applications.

Commercial polyurethane (PUR) foams were selected as sacrificial templates owing to their highly interconnected open-cell structure and excellent flexibility. Two PUR foams with different pore sizes were used to investigate the influence of template morphology on the final metallic architecture (Fig. 10). Each foam was cut into rectangular specimens measuring approximately 3 × 1 cm, ensuring identical dimensions for all samples.

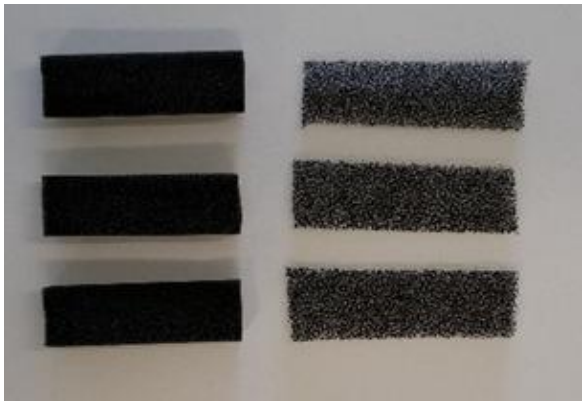


Figure 10. PUR foam templates with different pore sizes used for the fabrication of nickel foams by the replication method.

To prepare the nickel coating slurry, 3 g of bovine skin gelatin (Sigma-Aldrich) was dissolved in 25 mL of ultrapure water under continuous magnetic stirring (350 rpm) at 45 °C. Gelatin was added gradually over approximately 10 min to ensure complete dissolution and to obtain a homogeneous binder solution. Subsequently, 18 g of nickel nanopowder (average particle size <100 nm, ≥99% trace metals basis, Sigma-Aldrich) was slowly incorporated into the gelatin solution while maintaining continuous stirring, producing a viscous suspension suitable for coating the polymer template (Fig. 11). Gelatin served as a temporary organic binder, improving the adhesion of nickel nanoparticles to the PUR framework during impregnation.

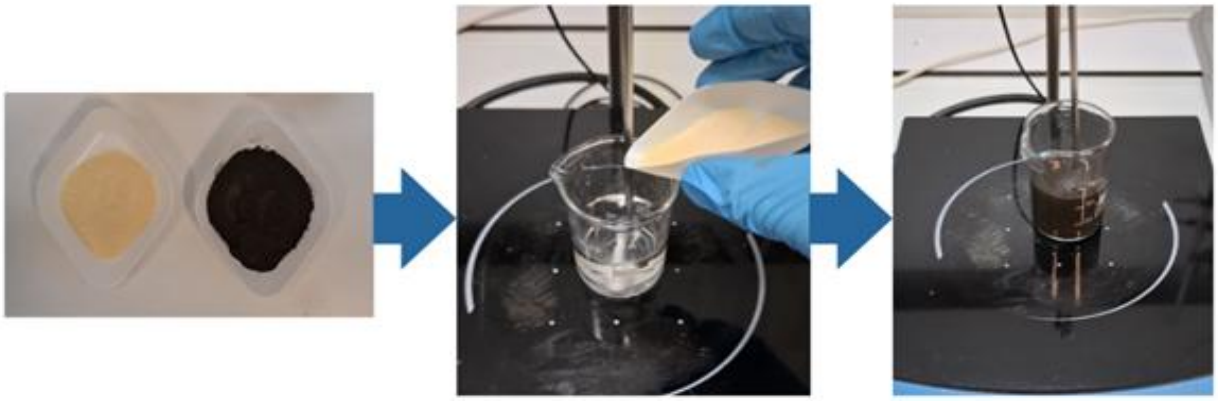


Figure 11. Preparation of the gelatin–nickel nanoparticle slurry used for impregnation of PUR templates.

The PUR templates were immersed in the nickel suspension to achieve complete infiltration of the open-cell structure. Following impregnation, the foams were placed on a Petri dish, and excess slurry was removed by gentle compression to prevent pore blockage while maintaining a uniform coating on the polymer skeleton. The impregnated foams were partially dried in a laboratory oven for 10 minutes before repeating the coating procedure. This impregnation–drying cycle was performed five times, ensuring sufficient loading of nickel nanoparticles throughout

the template. After the final coating, the samples were dried at 50 °C for 3 h to remove residual moisture and stabilize the deposited nickel coating (Fig. 12).

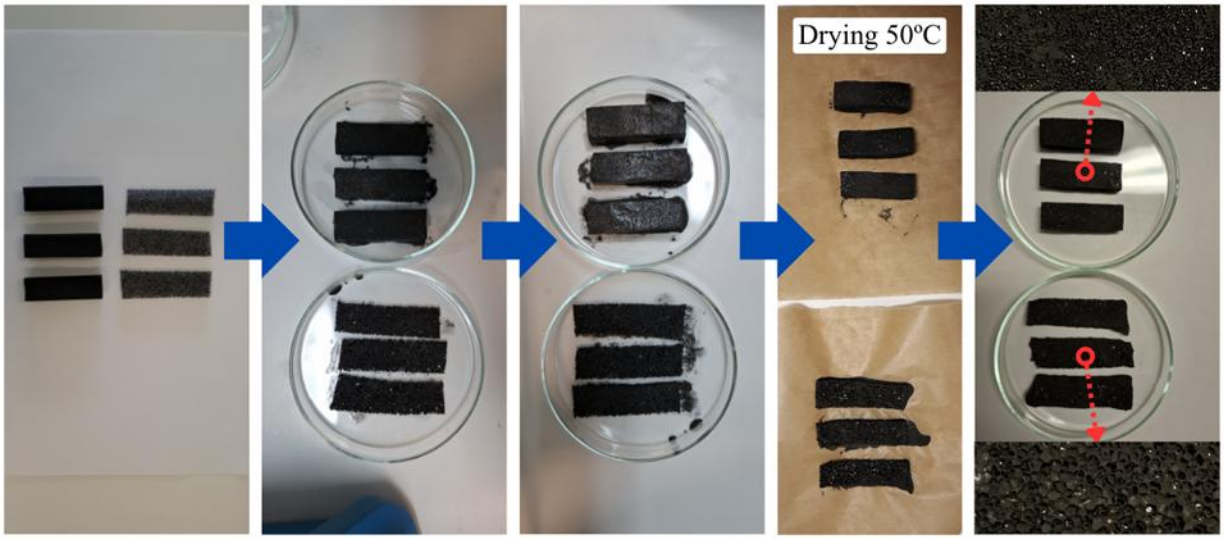


Figure 12. Sequential impregnation and drying of PUR foam templates with the nickel nanoparticle slurry showing uniform coating of the open-cell structure.

The dried nickel-coated PUR templates were subsequently subjected to thermal processing in a programmable quartz tube furnace. The first stage consisted of controlled thermal debinding in a nitrogen atmosphere to remove the polymer template without damaging the fragile metallic network. A multistep heating program was employed to gradually decompose the polyurethane and minimize shrinkage and cracking of the green metallic skeleton. Initially, the samples were heated to 120 °C at a rate of 1 °C min^{-1} and held for 1 h. The temperature was then increased to 250 °C at 0.5 °C min^{-1} with a holding time of 1 h, followed by heating to 425 °C at the same heating rate and maintained for 2 h. This slow thermal decomposition enabled complete removal of the polymer template while preserving the three-dimensional porous architecture.

Following debinding, the remaining nickel nanoparticle network was consolidated by sintering under a flowing hydrogen atmosphere. The samples were

heated to 700 °C at a rate of 8 °C min^{-1} and held for 1 h. The reducing atmosphere simultaneously removed surface nickel oxides and promoted particle necking and densification, resulting in mechanically stable metallic foams with continuous conductive pathways (Fig. 13). The final products were self-supporting nickel foams faithfully replicating the morphology of the original polyurethane templates.

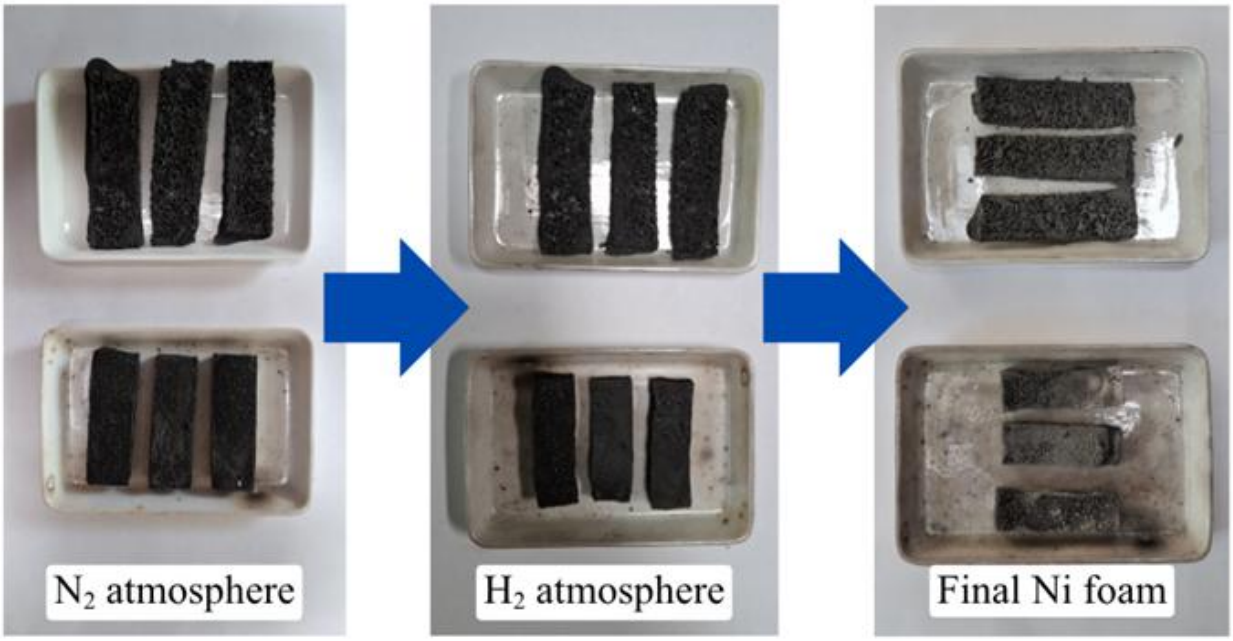


Figure 13. Fabrication of porous nickel foams by thermal treatment. The process includes controlled thermal debinding of the polyurethane template under N_2, hydrogen-assisted sintering, and the resulting self-supporting porous Ni foam.

The replication method produced lightweight, highly porous nickel foams characterized by an interconnected open-cell structure, high electrical conductivity, and large electrochemically accessible surface area. Owing to these structural characteristics, the fabricated Ni foams are well suited as binder-free electrodes and catalyst supports for hydrogen evolution and other electrochemical reactions. Furthermore, the use of two polyurethane templates with different pore sizes enables

systematic evaluation of the influence of pore architecture on the morphology, mechanical integrity, and catalytic performance of the resulting nickel foams.

1.8 Valorization of PUR foams into an efficient HER catalyst by electroless deposition and electrodeposition of Ni

Commercial open-cell polyurethane (PUR) foam was employed as a low-cost three-dimensional template for the fabrication of porous nickel electrodes for the HER. Owing to its highly interconnected open-cell architecture, low density, and excellent mechanical flexibility, PUR foam provides an ideal scaffold for the preparation of self-supported metallic catalysts with high specific surface area and efficient electrolyte transport. The fabrication strategy was based on the sequential transformation of an electrically insulating polymer into a conductive and catalytically active nickel framework through graphite coating, electroless nickel deposition, and electrochemical nickel deposition from a deep eutectic solvent (DES)-based electrolyte. The overall preparation procedure is illustrated in Fig. 14.

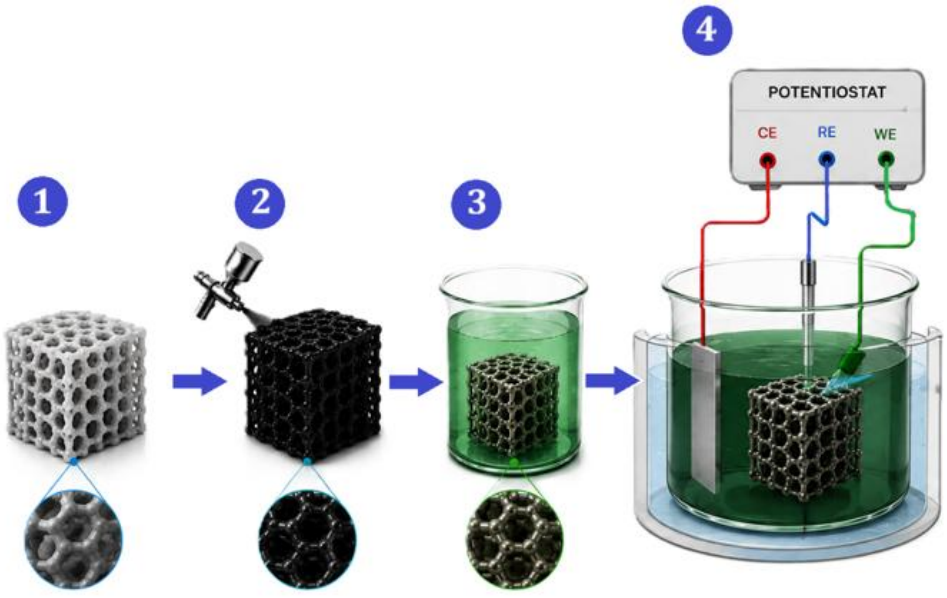


Figure 14. Schematic illustration of the experimental procedure for fabrication of Ni-coated PU foam: (1) pristine PU foam; (2) graphite spray coating; (3) electroless

Ni deposition from an aqueous solution; (4) electrochemical Ni deposition from a DES-based electrolyte.

Initially, commercial PUR foam was cut into specimens of the required dimensions, cleaned with isopropanol to remove surface contaminants, and dried under ambient conditions. Since polyurethane is electrically insulating, a conductive surface layer was created by applying a commercially available graphite spray (Graphit 33, Kontakt Chemie). The graphite coating was deposited uniformly over the entire polymer skeleton in three successive spraying cycles, allowing complete solvent evaporation between each application. This simple conductive pretreatment eliminated the need for conventional Pd/Sn sensitization and activation procedures typically required for metallization of polymer substrates, while preserving the original porous architecture of the foam. After the final coating, the graphite-covered PUR foam was dried at room temperature before further processing.

The conductive graphite-coated PUR foam was subsequently metallized by electroless nickel deposition. The electroless plating bath consisted of nickel sulfate hexahydrate as the nickel source, sodium hypophosphite monohydrate as the reducing agent, sodium citrate as the complexing agent, and sodium acetate as the buffering agent. The composition and operating parameters of the plating bath are summarized in Table 5. During deposition, the graphite-coated PUR foam was immersed in the plating solution maintained at 80–90 °C and pH 4.8 for 60 min under continuous magnetic stirring to ensure uniform nickel deposition throughout the three-dimensional porous structure. Upon completion of the process, the samples were rinsed thoroughly with deionized water and dried. The chemically deposited nickel layer formed a continuous conductive coating on the polymer skeleton and served as a metallic seed layer for the subsequent electrochemical deposition process.

Table 5. Composition and operating conditions of the electroless nickel plating bath.

Parameter	Value
$NiSO_4 \cdot 6H_2O$	25 g L^{-1}
$NaH_2PO_2 \cdot H_2O$	25 g L^{-1}
Sodium citrate	20 g L^{-1}
Sodium acetate	10 g L^{-1}
pH	4.8
Operating temperature	80–90 °C
Deposition time	60 min

To further increase the nickel loading and develop a highly active catalytic surface, an additional nickel layer was deposited electrochemically from a DES-based electrolyte. The electrolyte was prepared from Ethaline, a 1:2 molar mixture of choline chloride and ethylene glycol, containing nickel chloride hexahydrate and boric acid, with the addition of 30 wt.% deionized water to adjust the electrolyte properties. The electrolyte composition and electrodeposition conditions are summarized in Table 6.

Table 6. Composition and operating conditions of the DES-based electrolyte for nickel electrodeposition.

Parameter	Value
$NiCl_2 \cdot 6H_2O$	1.0 M
Boric acid	0.13 M
Additional water	30 wt.%
Ethaline	Balance
Applied potential	−1.0 V

Operating temperature	40 °C
Deposition time	20 min

Nickel electrodeposition was performed potentiostatically using an Autolab PGSTAT302N potentiostat in a thermostatically controlled three-electrode electrochemical cell maintained at 40 °C. The electroless nickel-coated PUR foam served as the working electrode, a nickel plate as the counter electrode, and a silver wire as the pseudo-reference electrode. Deposition was carried out at an applied potential of −1.0 V for 20 min, after which the samples were rinsed with deionized water and dried under ambient conditions.

The combination of graphite coating, electroless nickel deposition, and DES-assisted electrodeposition enabled the conversion of inexpensive commercial PUR foam into a mechanically stable, electrically conductive, and highly porous nickel electrode while preserving the original interconnected open-cell structure. Graphite coating provided sufficient electrical conductivity for subsequent metallization, electroless deposition generated a continuous nickel framework over the entire polymer skeleton, and electrodeposition from the DES-based electrolyte substantially increased the nickel loading and produced a highly developed hierarchical nickel surface. The overall fabrication strategy offers a simple, scalable, and cost-effective route for the valorization of commercial PUR foams into self-supported nickel electrocatalysts with significant potential for hydrogen evolution and other electrochemical energy-conversion applications. The successive stages of the fabrication process and the visual transformation of the PUR foam during metallization are presented in Fig. 15.

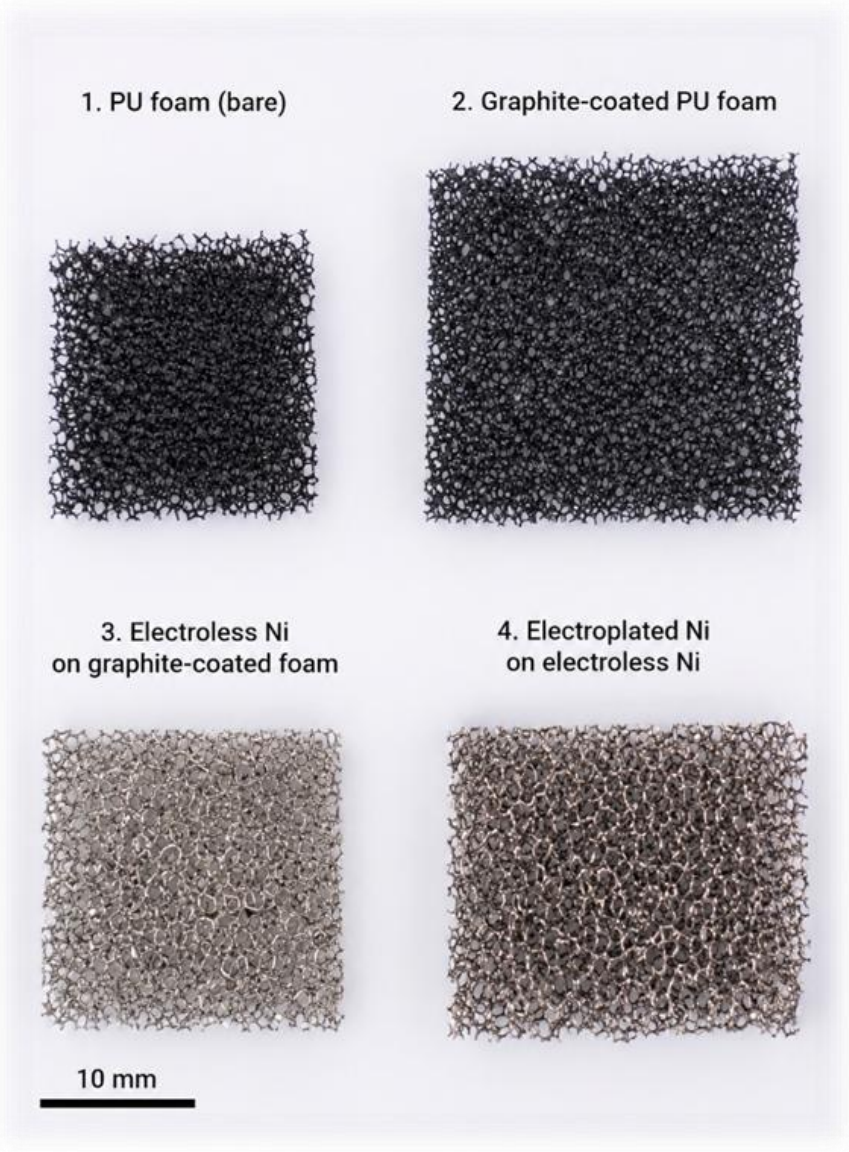


Figure 15. Visual appearance of the polyurethane (PUR) foam at successive stages of the metallization process: (1) bare PU foam, (2) graphite-coated PU foam, (3) electroless Ni-coated graphite-covered PU foam, and (4) electrochemically deposited Ni coating on the electroless Ni layer. The photographs demonstrate the progressive change in surface morphology and appearance associated with each processing step.

1.9 Electrodeposition and process optimization of Ni/M-Xene composite catalytic coatings

Electrodeposition of Ni/M-Xene coatings was carried out using an electrolyte with the composition specified in Table 7. The electrodeposition process was performed at temperatures ranging from 30 to 60 °C in a conventional three-electrode electrochemical cell, as described previously in Section 1.4.3. Copper (Cu) substrates were used as catalyst holders. Before deposition, the substrates underwent a thorough cleaning procedure involving degreasing and etching. All samples were subjected to electrodeposition at current densities ranging from 5 to 25 mA/cm² for 20 minutes.

Table 7. Composition and operating conditions of the DES-based electrolyte for Ni/M-Xene electrodeposition.

Parameter	Value
$NiCl_2 \cdot 6H_2O$	1.0 M
Boric acid	0.13 M
Additional water	30 wt.%
Ethaline	Balance
Applied current density	5 – 25 mA/cm^2
Operating temperature	30 – 60 °C
Deposition time	20 min

All obtained samples exhibited an attractive appearance and a homogeneous surface, with colors ranging from light metallic to dark gray depending on the applied current density and deposition temperature. The coatings were smooth and of good overall quality, with no visible cracks or other surface defects. Detailed

information on coating weight, thickness, and deposition rate is presented in Table 8.

Table 8. Coating weight, thickness, and deposition rate of Ni/M-Xene coatings obtained at different electrodeposition conditions.

Electrodeposition temperature, ^{o}C	Applied current density, mA/cm^2	Coating weight m, mg	Thickness, μm	Deposition rate DR, μm/min
30	5	6.5	1.82	0.0912
	10	14.4	4.04	0.202
	15	20.6	5.78	0.289
	20	28.5	8.00	0.400
	25	35.2	9.88	0.494
40	5	7.1	1.99	0.100
	10	14.5	4.08	0.204
	15	19.8	5.56	0.278
	20	28.8	8.09	0.405
	25	36.0	10.1	0.505
50	5	8.4	2.36	0.118
	10	14.8	4.16	0.208
	15	21.2	5.95	0.298
	20	30.8	8.65	0.433
	25	36.9	10.36	0.518
60	5	8.6	2.41	0.121
	10	16.2	4.55	0.228

	15	22.2	6.23	0.312
	20	31.2	8.75	0.438
	25	37.0	10.39	0.520

The experimental results demonstrate that the applied current density had a pronounced effect on the amount of deposited material and, consequently, on the thickness and deposition rate of the Ni/M-Xene coatings. At all investigated temperatures, increasing the current density from 5 to 25 mA/cm² resulted in a substantial and nearly systematic increase in coating thickness and deposition rate. This behavior is consistent with the expected increase in the rate of electrochemical reduction and matrix growth when a higher cathodic current is applied.

The combined influence of current density and electrolyte temperature on the deposition rate is illustrated in Figure 16. The deposition rate increased predominantly with increasing current density, while an additional positive effect of temperature was also observed. At 30 °C, the deposition rate increased from approximately 0.091 μm/min at 5 mA/cm² to 0.494 μm/min at 25 mA/cm². At 60 °C, the corresponding values increased from approximately 0.121 to 0.520 μm/min. Thus, the effect of current density was substantially stronger than the effect of temperature within the investigated experimental range.

The moderate increase in deposition rate with increasing temperature can be associated with changes in the transport properties of the DES-based electrolyte. Increasing temperature decreases electrolyte viscosity and facilitates ionic transport, thereby improving the supply of electroactive nickel species to the cathode surface. Enhanced mass transport becomes particularly relevant at higher current densities, where the consumption rate of electroactive species at the electrode/electrolyte interface is increased.

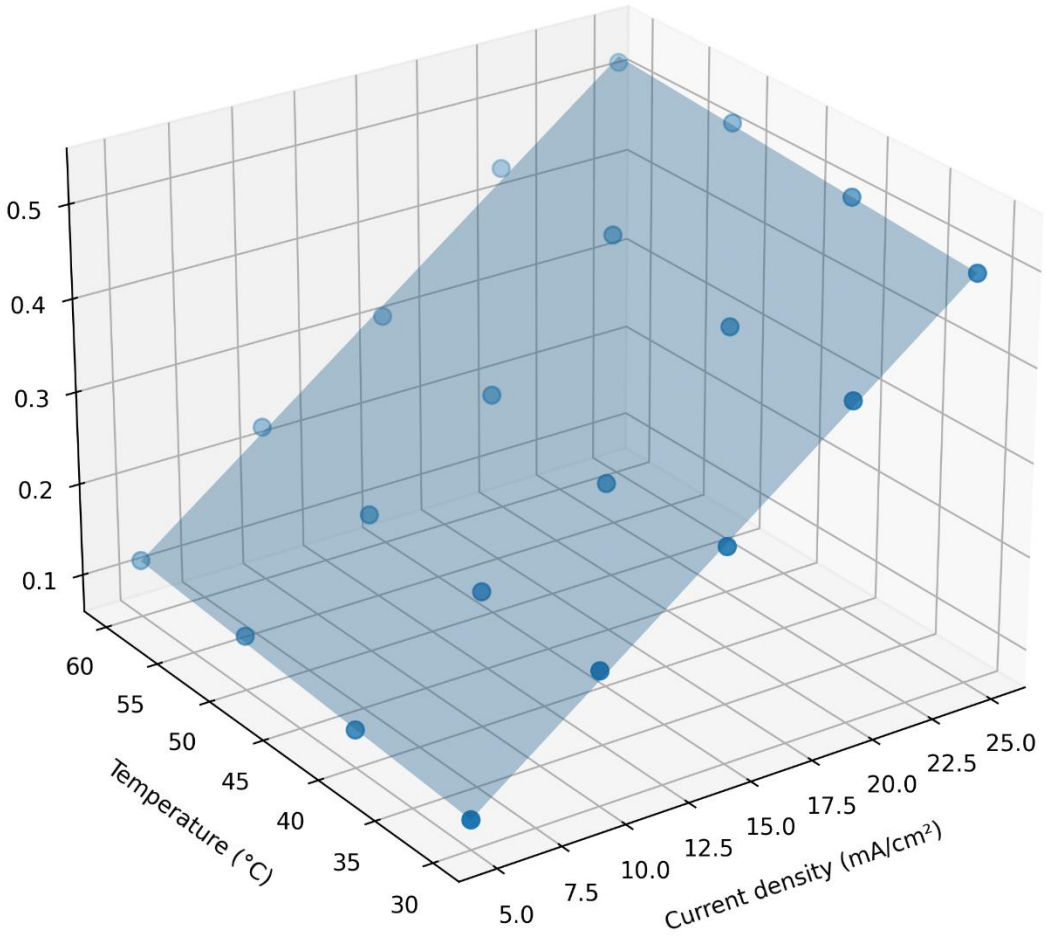


Figure 16. Effect of electrodeposition temperature and applied current density on the deposition rate of Ni/M-Xene coatings.

To obtain further insight into the electrochemical behavior of the Ni/M-Xene deposition process, the electrode potential was monitored during galvanostatic electrodeposition. After stabilization of the potential, representative quasi-stationary values were determined for each applied current density and electrolyte temperature. These values are summarized in Table 9 and were subsequently used to construct the quasi-stationary polarization curves shown in Figure 17.

Table 9. Electrode potentials during Ni/M-Xene electrodeposition at different temperatures and applied current densities.

Electrodeposition temperature, °C	**Applied current density, -j, mA/cm²**	**Potential, V**
30	5	**−0.744**
	10	**−0.913**
	15	**−1.038**
	20	**−1.180**
	25	**−1.305**
40	5	**−0.595**
	10	**−0.73**
	15	**−0.81**
	20	**−0.91**
	25	**−1.010**
50	5	**−0.558**
	10	**−0.658**
	15	**−0.738**
	20	**−0.790**
	25	**−0.858**
60	5	**−0.518**
	10	**−0.603**
	15	**−0.695**
	20	**−0.753**
	25	**−0.818**

The data presented in Table 9 show a clear dependence of the deposition potential on both applied current density and electrolyte temperature. At each investigated temperature, increasing the current density shifted the electrode potential toward progressively more negative values. For example, at 30 °C the potential changed from −0.744 V at 5 mA/cm² to −1.305 V at 25 mA/cm². This increase in cathodic polarization reflects the greater electrochemical driving force required to sustain the higher rate of metal reduction and coating growth.

Temperature produced the opposite effect. At a constant current density, increasing the electrolyte temperature generally shifted the deposition potential toward less negative values. At 5 mA/cm², for example, the potential changed from −0.744 V at 30 °C to −0.518 V at 60 °C. Similarly, at 25 mA/cm², the potential shifted from −1.305 V at 30 °C to −0.818 V at 60 °C. These results indicate a substantial reduction in cathodic polarization with increasing electrolyte temperature.

The quasi-stationary polarization curves constructed from these data are presented in Figure 17. The systematic displacement of the curves toward less negative potentials with increasing temperature confirms that the Ni/M-Xene electrodeposition process becomes electrochemically more favorable at elevated temperatures. This behavior can be attributed primarily to reduced viscosity of the DES-based electrolyte, enhanced ionic conductivity, improved mass transport of nickel-containing species, and accelerated charge-transfer processes at the electrode/electrolyte interface.

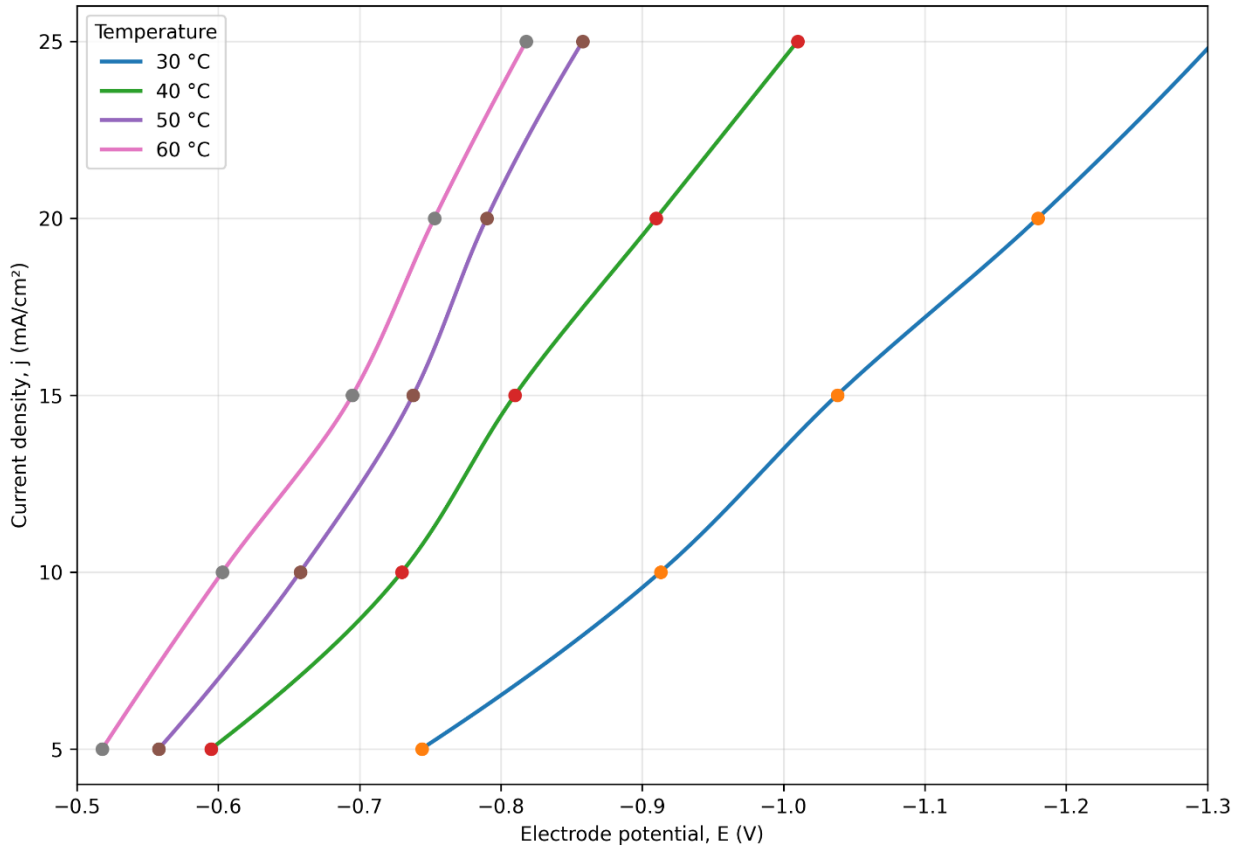


Figure 17. Quasi-stationary polarization curves for Ni/M-Xene coating electrodeposition at different electrolyte temperatures.

Comparison of Figures 16 and 17 provides a more complete description of the Ni/M-Xene electrodeposition process. Increasing current density strongly accelerates coating growth but simultaneously requires progressively greater cathodic polarization. Increasing temperature, in contrast, moderately enhances the deposition rate while considerably decreasing the magnitude of the cathodic potential required to maintain a given current density. Temperature therefore improves the electrochemical conditions for deposition by facilitating charge transfer and mass transport within the DES-based electrolyte.

The results demonstrate that both current density and temperature can be effectively used to control the electrodeposition of Ni/M-Xene coatings. Current density primarily determines coating growth rate and thickness, whereas temperature has a particularly pronounced influence on the electrochemical polarization of the deposition process. The investigated parameter range provides stable formation of homogeneous Ni/M-Xene coatings and establishes a basis for selecting deposition conditions according to the required catalyst loading, coating thickness, and electrochemical characteristics.

1.10 Synthesis of $Ni_{1-x}Co_xS$ Electrocatalysts and Electrode Fabrication

A series of $Ni_{1-x}Co_xS$ compositions (x =0.1, 0.25, 0.4, 0.5, and 0.6) was synthesized in a mixer mill (MM 500, Retsch, GmbH, Haan, Germany) using a 125 mL stainless steel (SS) milling chamber equipped with an integrated pressure and temperature sensor (GrindControl, Retsch, GmbH, Haan, Germany). Elemental Ni, Co, and S powders were mixed in stoichiometric ratios corresponding to the target composition. Two particle-size types of Ni and Co were used to evaluate the effect of precursor size on MSR ignition.

For all syntheses, 5 g of powder was loaded into the milling chamber together with 32 SS milling balls with a diameter of 10 mm, resulting in a ball-to-powder ratio (BPR) of 37:1. Milling was performed in an air atmosphere at 30 Hz, with the milling time depending on MSR ignition but not exceeding 30 s. MSR ignition was identified by a rapid increase in pressure and a short, sharp acoustic signal characteristic of an MSR event, after which milling was immediately stopped.

For comparison, monometallic sulfides were also synthesized using fine Ni and Co powders. NiS was successfully prepared under the same conditions as the $Ni_{1-x}Co_xS$ series. In contrast, CoS could not be obtained using the same MSR protocols as the bimetallic samples and was therefore synthesized in a planetary mill

(Pulverisette 7, Fritsch GmbH, Idar-Oberstein, Germany) at 500 rpm using tungsten carbide (WC) media (80 mL WC chamber, 25 WC balls with 10 mm diameter, and BPR of 37:1). In the following discussion, these experimentally synthesized monometallic samples will be referred to as the NiS and CoS reference samples. These should be distinguished from the reference phases taken from the ICDD database, which are used for phase identification (i.e. e. g., Ni_7S_6, Ni_8S_9, NiS, NiS_2, Co_9S_8, CoS).

In addition, it should be emphasized that all samples were used as- synthesized without additional treatments such as washing or calcination.

Catalyst inks were prepared by dispersing 50 mg of the synthesized material in a solvent mixture containing 800 μL of isopropanol (IPA) and 200 μL of deionized water. The dispersion was ultrasonicated for 30 min to ensure homogeneity. Before use, the GCE, diameter 5 mm, was electrochemically cleaned by cycling in 0.5 M H_2SO_4 over a potential range of -1 to 1 V vs. Ag/AgCl (3 M KCl) at a scan rate of 100 mV s^{-1} and then rinsed with ultrapure water. A total of 20 μ L of the resulting ink (2 ×10 μL) was drop-cast onto a GCE and allowed to dry under ambient conditions. The resulting catalyst mass on the GCE was 1 mg, corresponding to a geometric loading of 5 mg cm^{-2}. After complete drying, a fixation layer was applied by drop-casting 10 μL of a Nafion-based binder solution (prepared by mixing 1 mL of IPA with 20 μL of Nafion). This layer served to enhance the adhesion and stability of the catalyst film during electrochemical testing.